**Bárbara Maria Machete Barradas**

Licenciatura em Bioquímica

# Protein Glycosylation in Cancer Drug Resistance

Dissertação para obtenção do Grau de Mestre
em Bioquímica para a Saúde

Orientador: Professor António Sebastião Rodrigues, PhD, ToxOmics, NOVA Medical School | Faculdade de Ciências Médicas da Universidade NOVA de Lisboa

Co-orientador: Professora Paula Videira, PhD, Glycoimmunology Group @ UCIBIO | NOVA SCHOOL OF SCIENCE AND TECHNOLOGY | FCT NOVA

**Dezembro, 2022**

## AGRADECIMENTOS

Finalizada mais uma etapa da minha vida, não poderia deixar de expressar o meu agradecimento a todos os que me apoiaram durante este ano e meio cheio de emoções. Foi um percurso desafiante que me proporcionou memórias que ficarão para o resto da vida, tanto a nível profissional como pessoal.

Ao meu orientador, Professor Doutor António Sebastião Rodrigues, quero agradecer por me receber no seu grupo e, tendo em conta todas as adversidades, por ter tornado possível a realização deste projeto. Agradeço todos os ensinamentos transmitidos, todo o apoio, disponibilidade e paciência ao longo do projeto e por nunca ter perdido esperança.

Ao Doutor Bruno Gomes, agradeço todas as horas dentro e fora do laboratório, a paciência que teve comigo, a ajuda incondicional sempre que precisei e todos os ensinamentos que partilhados. Não chegaria aqui sem a sua ajuda.

À Doutora Susana Silva e Francisco Esteves, obrigada por todas as palavras de motivação e pela prontidão em ajudar em qualquer situação.

Ao Professor José Rueff, por me aceitar no Centro de Toxicogenómica e Saúde Humana (ToxOmics).

À Doutora Júlia Costa pela disponibilidade e contribuição nas experiências de western blot.

À minha coorientadora, Professora Paula Videira e à Doutora Daniela Barreira, obrigada pelos conhecimentos transmitidos.

A todas as minhas colegas de laboratório, Andreia Chande, Catarina Duarte, Matilde Vale, Joana Amorim, Diana Sousa, Jhenifer Oliveira, Isabel Barata, Mariana Pereira, Marta Santos obrigada do fundo do coração pelo apoio quase diário, perto ou longe, pelos cafés, pelas cantorias, pelas conversas, por tudo!

Aos de sempre João Bandadas, Madalena Salgueiro e Maria Nunes, obrigada por estarem presentes em mais uma etapa da minha vida, certamente estarão presentes nas próximas, não tenho palavras suficientes.

Por fim, não menos importante, um grande agradecimento à minha família. Em especial, aos meus pais pelo apoio constante.

A todos, um grande obrigada!

## ABSTRACT

Breast Cancer (BC) is acknowledged as the world's most prevalent cancer and the second cause of death worldwide. This disease comprises several cellular modifications and presents molecular heterogeneity, due to its' genomic instability. Despite the advances in therapy, resistance to chemotherapeutic agents remains one of the major obstacles in cancer treatment – 90% of failures in chemotherapy are related to chemoresistance in metastatic cancer. Various mechanisms underlie cancer drug resistance (CDR), and aberrant glycosylation has emerged as a further hallmark of cancer. Protein glycosylation is the most abundant posttranslational modification (PTM) catalysed by different coordinated glycosyltransferases and glycosidases. This process has long been associated with the development and progression of cancers and its dysregulation leads to an aberrant glycosylation pattern in tumour cells, however, the mechanistic basis remains poorly explained. The main modifications in tumour-associated structures are increased glycan branching, sialylation, and fucosylation, along with novel or truncated glycan structures.

In this project, we verified the role of glycosylation in CDR, specifically in paclitaxel (PAX) resistant cells. Previous work in our lab developed a PAX-resistant cell line (MDA-MB-231/PAX), which allowed the analysis of differential protein glycosylation patterns in MDA-MB-231/400nM, MBA-MB-231/1000nM and PAX-sensitive BC cells and to understand whether glycosylation is a feature of PAX resistance. Changes in glycosylation patterns were detected by western blot, our data suggest that altered glycosylation in cell's glycocalyx occurs during the development of resistance to PAX in BC. To evaluate changes in glycosylation gene expression we carried out RT-PCR assays, two genes were identified as possible biomarkers of PAX resistance in BC cells, *GALNT14* and *MGAT3*.



**Keywords:** Breast Cancer (BC); Cancer Drug Resistance (CDR); Paclitaxel (PAX); Aberrant Glycosylation; Glycans; Cancer Biomarkers;

## RESUMO

Cancro da mama (CM) é conhecido como o cancro mais predominante no mundo e a segunda causa de morte a nível mundial. Esta doença desenvolve várias modificações celulares e apresenta heterogeneidade molecular, devido à sua instabilidade genómica. Apesar dos avanços terapêuticos, a resistência a agentes quimioterapêuticos continua a ser um dos principais obstáculos no tratamento do cancro - 90% das adversidades quimioterapêuticas estão relacionadas com a quimioresistência em cancro metastático. Vários mecanismos estão subjacentes à resistência a fármacos contra o cancro (RFC), porém a glicosilação aberrante é outra característica do cancro. A glicosilação é a modificação pós-traducional mais abundante, catalisada por diferentes e coordenadas glicosiltransferases e glicosidases. Este processo tem sido associado com o desenvolvimento e a progressão do cancro e a desregulação deste processo biológico desencadeia um padrão de glicosilação aberrante nas células tumorais, no entanto, a base mecanística permanece pouco desenvolvida. As principais modificações nas estruturas dos glicanos associados a tumores são o aumento da ramificação de glicanos, a sialilação e a fucosilação, juntamente com novas estruturas ou ainda estruturas de glicanos incompletas.

Neste projeto, verificámos a função que o processo de glicosilação possui na RFC, especificamente em células resistentes ao paclitaxel (PAX). Anteriormente no nosso laboratório, foi desenvolvida uma linha de células resistentes a PAX (MDA-MB-231/PAX), que permitiu a análise de padrões diferenciais de glicosilação em células MDA-MB-231/400nM, MBA-MB-231/1000nM e sensíveis ao PAX e assim compreender se a glicosilação é uma característica crítica da resistência ao PAX. Alterações nos padrões de glicosilação foram detetadas por western blot, os nossos dados sugerem que durante o desenvolvimento de resistência ao PAX, o glicocálice das células de CM está alterado. Para avaliar alterações na expressão dos genes de glicosilação realizámos ensaios de RT-PCR, tendo sido identificados dois genes como possíveis biomarcadores de resistência ao PAX nestas células, GALNT14 e MGAT3.



**Palavras-chave:** Cancro da mama (CM); resistência a fármacos contra o cancro (RFC); Paclitaxel (PAX); Glicosilação aberrante; Glicanos; Biomarcadores de cancro;

## LIST OF ABBREVIATIONS

ABC – ATP-Binding Cassette
ABCB1 – ATP-Binding Cassette Subfamily B Member 1 | P-glycoprotein
ABCC1 – ATP-Binding Cassette Subfamily C Member 1 | Multidrug Resistance-Associated Protein 1
ABCG2 – ATP-Binding Cassette Subfamily G Member 2 | Breast Cancer Resistance Protein
Asn – Asparagine
BC – Breast Cancer
Bcl-2 – B-cell lymphoma 2
BRCA1 – Breast Cancer gene 1
BRCA2 – Breast Cancer gene 2
BSA – Bovine Serum Albumin
CA – Cancer Antigen
CDR – Cancer Drug Resistance
CYP – Cytochrome P450
DDR – DNA Damage Response
DMEM – Dulbecco's Modified Eagle's Medium
ECM – Extracellular Matrix
EDTA –Ethylenediamine tetraacetic acid
EGFR – Epidermal Growth Factor Receptor
EMT – Epithelial-Mesenchymal Transition
ER – Endoplasmic Reticulum
ER – Estrogen Receptor
ERK - Extracellular Regulated Kinase
FBS - Fetal Bovine Serum
FOXM1 – Forkhead box protein M1
Fuc – Fucose
FUT8 – Fucosyltransferase 8
FUTs – Fucosyltransferases
Gal – Galactose
GALNTs - N-acetylgalactosaminyltransferases
GALNT14 – Polypeptide N-Acetylgalactosaminyltransferase 14

GBP – Glycan-Binding Proteins

Glc – Glucose

GlcA – Glucuronic Acid

GalNAc – N-acetylgalactosamine

GALNT6 – Polypeptide N-Acetylgalactosaminyltransferase 6

GlcNAc – N-acetylglucosamine

GlcNAcT-V – N-Acetylglucosaminyltransferase V

HER2 – Human Epidermal Growth Factor Receptor 2

HNK-1 – Human Natural Killer-1

$Le^a$ – Lewis A

$Le^x$ – Lewis X

Man – Mannose

mAB – Monoclonal antibodies

Mcl-1 – Myeloid leukemia 1

MGAT3 – Beta-1,4-Mannosyl-Glycoprotein 4-Beta-N-Acetylglucosaminyltransferase

MGAT5 – Alpha-1,6-Mannosylglycoprotein 6-Beta-N-Acetylglucosaminyltransferase

MDR – Multidrug Resistance

miRNA - MicroRNA

NCI - National Cancer Institute

OST – Oligosaccharyltransferase

OGT – O-GlcNAc transferase

PAS – Periodic Acid-Schiff

PAX – Paclitaxel

PBS – Phosphate-buffered saline

PD-L1 – Programmed cell Death Ligand 1

PR – Progesterone Receptor

Pro – Proline

ppGALNAc-T – Polypeptide N-Acetylgalactosaminyltransferase

PTM - Posttranslational Modification

PVDF – Polyvinylidene fluoride

RT – Room Temperature

RT-PCR – Real-Time-Polymerase chain reaction

SDS-PAGE – Sodium Dodecyl Sulfate-Polyacrylamide Gel Electrophoresis

Ser – Serine

SEM – Standard Error of the Mean

Sia – Sialic Acid | Neu5Ac

SIRT1 – Sirtuin 1

sLe$^{a}$ - Sialyl Lewis A

sLe$^{x}$ – Sialyl Lewis X

ST6GAL1 – ST6 Beta-Galactoside Alpha-2,6-Sialyltransferase 1

STn – Sialyl Thomsen-nouveau

TACAs – Tumour-Associated Carbohydrate Antigens

TCGA – The Cancer Genome Atlas

TGF-β – Transforming Growth Factor beta

TGN – *trans*-Golgi network

Thr – Threonine

Tn – Thomsen-nouveau

TNBC – Triple Negative Breast Cancer

TRAIL – Tumour Necrosis Factor-Related Apoptosis-Inducing Ligand

Xyl – Xylose

WHO – World Health Organization

## TABLE OF CONTENTS

## LIST OF FIGURES

## LIST OF TABLES

# 1. INTRODUCTION

## 1.1 BREAST CANCER

According to the World Health Organization (WHO), Breast Cancer (BC) is acknowledged as the world's most prevalent cancer, reflected in 2020 statistics, where 2.3 million women were diagnosed with BC and 685000 deaths were estimated globally. Cancer is the second leading cause of death worldwide (Ritchie, Spooner e Roser, 2018) and BC is the most commonly occurring cancer in women (Ferlay *et al.*, 2021). In Portugal, 7041 new cases were registered in 2020 (26,4% of all new cases in women of all ages), becoming the most common cancer among Portuguese women (Global Cancer Observatory, 2022). Considering the numbers predicted by the Global Cancer Observatory, the incidence and mortality of BC will continue rising. In 2040 3.19 million new cases are estimated worldwide (Global Cancer Observatory, 2022).

Cancers are defined by the US National Cancer Institute (NCI) as a compilation of diseases in which abnormal or damaged cells grow uncontrollably and can spread to nearby tissue. These cells form neoplasms, also called tumours, which are masses of tissue and can be cancerous (malignant) or not cancerous (benign). Cancer occurs as a result of several gene mutations, inducing the dysfunction of vital genes and generating cancerous features in normal cells and therefore altering cell's functions.

BCs are defined by where in the breast they begin to grow, with most of them being carcinomas, which are tumours that initiate in the epithelial cells. According to the latest edition of the WHO classification, breast carcinomas are divided into 19 different major subtypes, including invasive carcinomas of no special type, also known as not otherwise specified, lobular carcinomas and the other carcinomas of a special type (including 17 different rare histotypes and their subclasses). BC of 'no special type' is a carcinoma that does not fit into a specific histotype (Harbeck *et al.*, 2019).

Notwithstanding, this is also a disease that presents molecular heterogeneity, due to its' genomic instability, thus tumour subtypes are classified through their protein expression, such as estrogen receptor (ER), progesterone receptor (PR), human epidermal growth factor receptor 2 (HER2) and the proliferation marker Ki67 (Table 1.1). Luminal A and Luminal B express ER and tumours expressing ER and/or PR are considered hormone receptor-positive BCs, whereas tumours not expressing ER, PR or HER2 are triple-negative BC (TNBC) (Harbeck *et al.*, 2019). Furthermore, included in these molecular features are *BRCA1* and *BRCA2* gene mutations. These genes are tumour suppressor genes and are the most common genes in autosomal dominant and high

penetrance forms of breast and ovarian cancer (Mehrgou e Akouchekian, 2016). The identification of BC susceptibility genes helps to establish and describe some aspects of this both sporadic and inherited disease.

**Table 1.1- Classification of molecular subtypes of breast cancer and the correspondent prognosis.** Source: (Harbeck *et al.*, 2019).

| **Breast Cancer Types** | | **Molecular features/ Biomarkers** | **Prognosis** |
|---|---|---|---|
| Invasive Breast Cancer<br><br>. Penetrates the neighbouring tissues and can metastasize to other body tissues and organs | Luminal A | $ER^{+}$, $PR^{+/-}$ and $HER2^{-}$; low Ki67 | Good |
| | Luminal B | $ER^{+}$, $PR^{+/-}$ and $HER2^{+/-}$; high Ki67 | Intermediate |
| | HER2 positive | $ER^{-}$, $PR^{-}$ and $HER2^{+}$; high Ki67 | Poor |
| | Triple-Negative (TNBC) | $ER^{-}$, $PR^{-}$ and $HER2^{-}$; high Ki67 | Poor |
| ER: estrogen receptor; PR: progesterone receptor; HER2: human epidermal growth factor receptor 2; -: negative; +: positive; | | | |

Studies have shown that the risk for BC is due to a combination of factors, such as age, gender, reproductive and family history, genetic mutations and lifestyle (more risk factors in *Panel 1* (Loibl *et al.*, 2021)). Establishing some alterations in a person's lifestyle can significantly reduce the risk of developing cancer. However, having a risk factor does not mean you will get this disease since most women have some risk factors, but do not develop BC according to the Division of Cancer Prevention and Control, Centers for Disease Control and Prevention.

**Panel 1: Risk factors for breast cancer**

- Personal history of breast lesions
- High breast density
- History of irradiation to the chest
- Type II diabetes
- Late pregnancy factors
- Low number of births or no pregnancy
- Short or no breastfeeding
- Obesity
- Alcohol intake
- Smoking
- Exposure to steroid hormones:

Hormonal therapy for climacteric symptoms
Recent oral contraceptives

## 1.2 CANCER DRUG RESISTANCE

Treatment strategies for this disease are wide-ranging and very often based on a combination of several approaches, depending on the tumours' stage and type and on the patients' tolerance. They include surgery, radiotherapy, and systemic therapy (endocrine therapy, chemotherapy, targeted therapy and immunotherapy) (Cheung, 2020). However, despite the advances in technology, resistance to chemotherapeutic agents and/or new targeted drugs remains one of the major obstacles in cancer treatment. In fact, 90% of failures in chemotherapy occur during the invasion and metastasis of cancers which is related to chemoresistance, resulting in disease relapse (Mansoori *et al.*, 2017). Hence the importance to better understand the mechanisms behind cancer drug resistance (CDR), to then develop highly efficacious therapies.

CDR can exist before treatment began or be generated during chemotherapy, intrinsic or acquired/extrinsic resistance, respectively. Intrinsic drug resistance can be induced in cancer cells due to inherent genetic alterations of genes involved in cancer cell growth and/or apoptosis (Wang, Zhang e Chen, 2019). The acquisition of resistance to chemotherapeutic agents by tumour cells involves several diverse and complex mechanisms such as enhanced or decreased drug efflux, drug inactivation, changes in drug metabolism, cell death inhibition (apoptosis suppression), multidrug resistance (MDR), enhancement in DNA repair capacity, tumour microenvironment features, epithelial-mesenchymal transition (EMT), epigenetic changes and gene amplification (Figure 1.1). These genomic instabilities are due to both genetic and epigenetic changes in tumour cells, which modify gene products through mutations, gene amplifications, deletions, chromosomal rearrangements, transposition of genetic elements, altered DNA methylation and histone modifications that are directly involved in CDR and poor prognosis, achieving the status of genetic heterogeneity in cancer (Chatterjee e Bivona, 2019; Haider *et al.*, 2020).

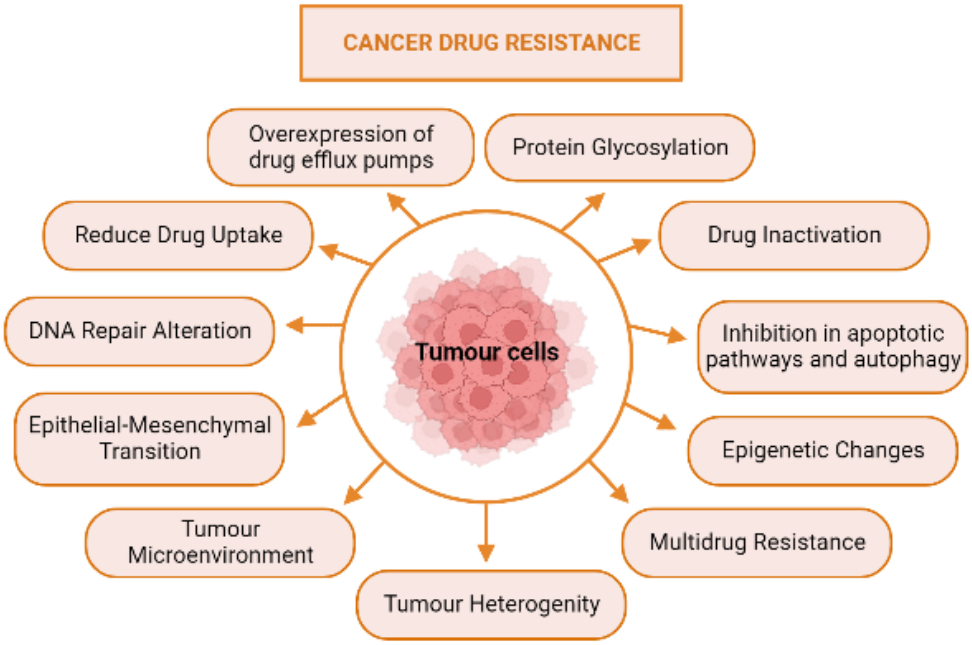


**Figure 1.1 – Mechanisms that promote direct or indirectly drug resistance in human cancer cells**. These mechanisms can act independently or in combination. Source: Haider et al., 2020. Created in BioRender.

Increased drug efflux has been considered to be one of the key mechanisms of CDR to chemotherapeutics since it leads to decreased levels of intracellular drug, as a result of abnormal high rates of outflow of anticancer agents (Wang, Zhang e Chen, 2019). The predominant transmembrane transporter proteins responsible for the enhanced efflux are from the ATP (adenosine triphosphate)-binding cassette (ABC) transporters superfamily. ABC drug transporters are composed by two cytoplasmic domains that bind to ATP and two transmembrane domains. The main function of these ABC transporters is to bind and hydrolyse the ATP molecule and to transfer the substrate across against the concentration gradient (Haider *et al.*, 2020). It is now known that the ABC transporter superfamily comprises at least 48 human genes with diverse functions and that they are overexpressed in cancer cells (Wang, Zhang e Chen, 2019). The ones highly involved in acquiring CDR in BC are P-glycoprotein (P-gp), multidrug resistance-associated protein 1 (MRP1) and Breast Cancer Resistance Protein (BCRP), which are referred to as ABCB1, ABCC1 and ABCG2, respectively (Figure 1.2).

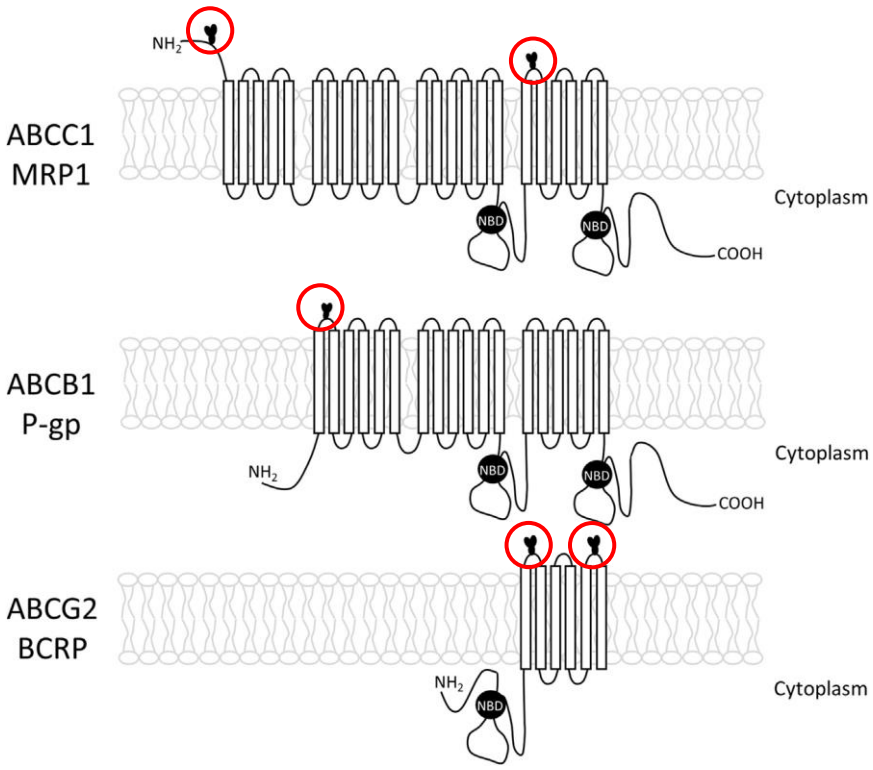


**Figure 1.2- Structure of the three main ABC transporters responsible for CDR in BC (ABCC1, ABCB1, and ABCG2), including transmembrane loops and their glycosylation sites**. N-glycosylation sites are circled in red. From: Fonseca *et al*., 2016.

ABCB1 and ABCG2 can efflux a wide variety of chemotherapeutic agents, including epipodophyllotoxins, anthracyclines, vinca alkaloids, bisantrene, colchicine, taxanes, imatinib, saquinavir, camptothecins, thiopurines, actinomycin D, methotrexate, and mitoxantrone, reducing intracellular drug accumulation (Bukowski, Kciuk e Kontek, 2020). ABCC1 also leads to resistance to several anticancer drugs, and extensive evidence indicates that resistance in cancer cells to mitoxantrone, saquinavir, epipodophyllotoxins, and anthracyclines is mediated by this transporter. The ABCG2 transporter is primarily expressed in BC, colon cancer, gastric cancer, small cell lung cancer, and ovarian cancer (Li *et al*., 2017).

MDR, as one of the hallmarks of cancer, includes several of the mechanisms mentioned above, such as increased drug efflux, drug inactivation, mutation in drug targets. It is defined as the resistance of cancer cells to multiple chemotherapeutic drugs with different structures and mechanisms of action. Many of these drugs require metabolic activation to became clinically successful. However, this is a complex process in which drugs interact with different proteins and in cancer cells this intercommunication is modified or partially degraded, developing resistance through drug inactivation (Longacre, Snyder e Sarkar, 2014). Moreover, targeted therapies are

much more effective and selective since they supress tumour growth and development through the inhibition of specific target proteins. Thus, drug effectiveness is determined by its molecular target and mutations or alterations in the target's expression due to epigenetic alterations alter anticancer drugs response and also leads to chemoresistance (Wang, Zhang e Chen, 2019). For example, topoisomerase II regulates DNA over- and underwinding, removing knots and tangles from the double helix and maintaining genomic integrity, yet certain anticancer drugs target resistant cells' topoisomerase II by stabilizing it which leads to DNA damage, inhibition of DNA synthesis and halting of mitotic processes. However, cancer cells may also develop resistance through mutations in the topoisomerase II gene (Longacre, Snyder e Sarkar, 2014). Indicating that the efficacy of DNA-damaging drugs depends on the cell's DNA damage response (DDR) mechanisms impairment or dysregulation since deregulation of DDR in non-diseased cells may precede chemoresistance. Mutations in determined genes and its consequent deterioration stimulate dysfunctional pathways and increase the DNA repair activity, increasing drug resistance (Haider *et al.*, 2020; Longacre, Snyder e Sarkar, 2014).

As mentioned, genomic instability, genetic defects in DNA repair genes and epigenetic changes play an important role in CDR. Epigenetic changes consist of several mechanisms such as DNA methylation, histone modification, chromatin remodelling, and noncoding RNA related alterations (such as microRNAs) which regulate gene expression throughout the chromosome. In cancer this regulation is altered, tumour suppressor genes are silenced via hypermethylation and oncogenes are over expressed through hypomethylation, affecting DDR and developing other mechanisms considered as hallmarks of cancer (Haider *et al.*, 2020; Wang, Zhang e Chen, 2019; Bukowski, Kciuk e Kontek, 2020).

Another important mechanism to consider in CDR is the epithelial to mesenchymal transition (EMT) by which solid tumours become metastatic, contributing pathologically to cancer progression. During EMT epithelial cells decrease the expression of cell adhesion receptors and increase the expression of receptors that induce cell motility, and acquire the characteristics of mesenchymal stem cells. This promotes the loss of cell-cell junctions and alters cell's morphology which stablishes invasive capacity. There are various contributes of EMT in the development of CDR, however, it depends on the metastatic grade of the tumour defined through the level of differentiation and degree of EMT (Haider *et al.*, 2020; Longacre, Snyder e Sarkar, 2014; Wang, Zhang e Chen, 2019).

### 1.2.1 CHEMOTHERAPEUTICS IN BREAST CANCER TREATMENT

Substantial development in BC treatment has been achieved in recent years, leading to the discovery of new drugs in cancer suppression and to the control of CDR progression. Treatment selection depends on tumour cells which are perceived as drug-sensitive or drug-resistant and can be performed through monotherapy or through a combination of numerous therapies, polytherapies, that target distinct resistance mechanisms, raising the chances of survival (Chatterjee e Bivona, 2019). Chemotherapeutics can be divided into two classes: plant-derived or synthetic origin (Bukowski, Kciuk e Kontek, 2020). Currently, there are several classes of chemotherapeutical drugs based on antimetabolites, alkylating agents, immunological elements, hormonal components, or mitotic deprivation (Samaan *et al.*, [s.d.]) (Table 1.2).

**Table 1.2- Chemotherapeutics' mechanisms of action used in systemic therapy in BC.** Adapted from: American Cancer Society Inc, 2022; (Samaan *et al.*, [s.d.]); Amboss; Cancer.org.

| CHEMOTHERAPEUTICS | MECHANISM OF ACTION |
|---|---|
| Antimetabolites | Interfere with a cell's RNA and DNA and are responsible for the induction of apoptosis during the synthesis phase.<br><br>E.g.: Fluorauracil; Methotrexate; Fludarabine; ... |
| Alkylating Agents | Damage DNA and block DNA replication. These drugs kill cells in all phases of the cell cycle.<br><br>E.g.: Chlorambucil; Cisplatin; Carboplatin; ... |
| Anthracyclines | Interfere with topoisomerases, which help separate the strands of DNA so they can be copied. Blocking the ability to mitosis and to repair damage to cells.<br><br>E.g.: Teniposide; Topotecan; ... |
| Antitumour Antibiotics | Anti-neoplastic drugs either break up DNA strands or slow down or stop DNA synthesis that cells require to proliferate.<br><br>E.g.: Bleomycin; Doxorubicin; ... |
| Mitotic inhibitors / Plant alkaloids | Intercept cells division but can damage cells in all phases by keeping enzymes from making proteins needed for cell reproduction.<br><br>E.g.: Paclitaxel; Vinblastine; ... |

#### 1.2.1.1 PACLITAXEL

Paclitaxel (PAX) is a chemotherapeutic drug, commercially denominated Taxol, and is inserted in the Taxanes class, with the empirical formula $C_{47}H_{51}NO_{14}$ (Figure 1.3). Taxanes are usually used in primary monotherapy or polytherapy treatment for patients with metastatic as well as early-stage BC, PAX is an antineoplastic drug that targets and alters microtubules' function and, consequently its stabilization (Samaan *et al.*, [s.d.]). Microtubules are tube-shaped protein polymers present in all eukaryotic cells composed of α and β-tubulin heterodimers in dynamic equilibrium, they are required for maintenance of cell structure, motility and cytoplasmatic movement within the cell. However, their main and crucial function is the formation of the mitotic spindle during cell division and mitosis, specifically at the prophase and the G2 phase of the cell cycle (Alqahtani *et al.*, 2019).

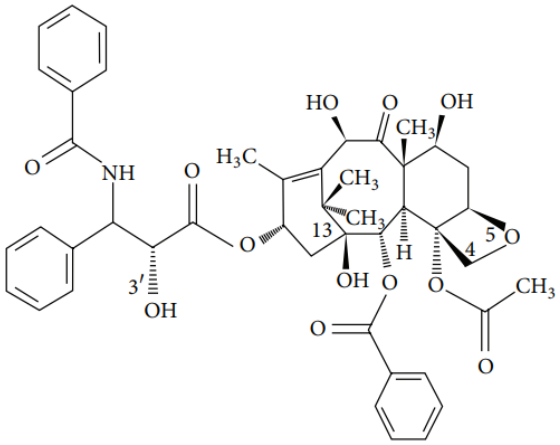


**Figure 1.3 – Chemical structure of Paclitaxel**. Source: Kampan *et al.*, 2015.

Accordingly, PAX inhibits cell proliferation since it blocks cell division and cells remain in the G2 phase (mitotic arrest) and eventually undergo apoptosis (Kampan *et al.*, 2015). This disruption in the cell cycle results from the binding of microtubules, repressing their depolymerization by promoting the assembly of α and β-tubulin subunits which interferes with microtubules' dynamics (Samaan *et al.*, [s.d.]).

The anti-tumour action mechanisms associated with PAX are many, such as activation of multiple proapoptotic signalling pathways that result in apoptosis, modulation of epigenetic markers through the alteration of some microRNAs (miRNAs) expression related with cancer growth and through the regulation of chemokines,

cytokines, or immune cells, in order to modulate immune responses. However, BC cells chemoresistant to PAX acquire distinct cellular and molecular mechanisms that lead to a disequilibrium in various signalling pathways, mutations in certain genes, e.g., overexpression of ABC transporters such as ABCB1, epigenetic deregulations such as DNA hypermethylation and PAX detoxification mediated by CYP (Figure 1.4). All this contributes to a worse clinical outcome for BC patients (Esparza-Lopez *et al.*, 2022; Maloney *et al.*, 2020; Němcová-Fürstová *et al.*, 2016; Samaan *et al.*, [s.d.]).

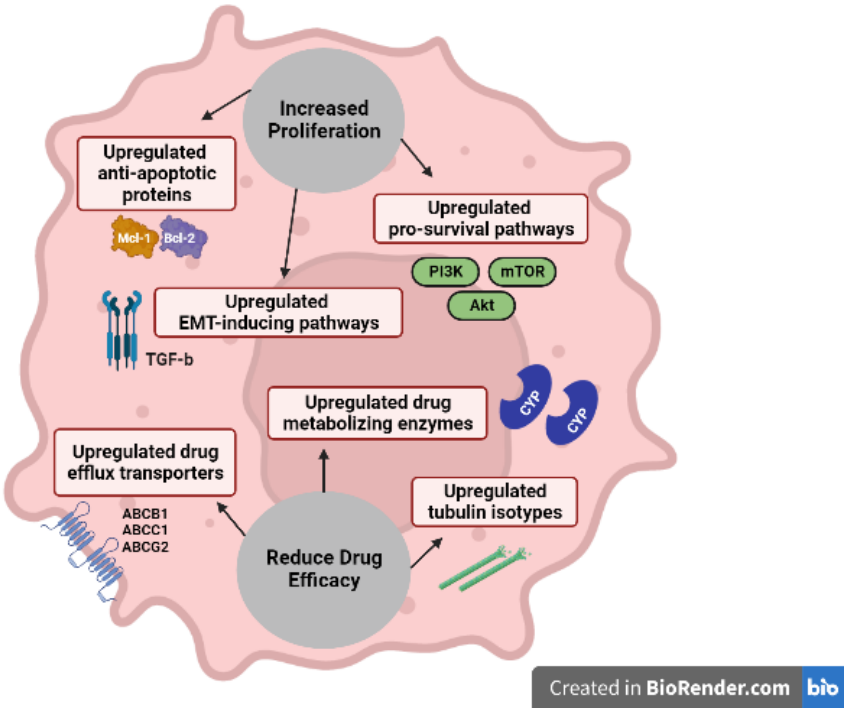


**Figure 1.4 – Illustration of some of the major taxane resistance mechanisms in BC.** Upregulated pro-survival pathways, upregulated EMT-inducing pathways (such as TGF-β) and upregulated anti-apoptotic proteins (such as Bcl-2 and Mcl-1) have been linked with increased proliferation after taxane treatment. The reduced taxane efficacy has been related to upregulated tubulin isotypes, increased drug efflux transporters and drug-metabolizing enzymes. Source: Maloney *et al.*, 2020. Created in BioRender.

## 1.3 GLYCOSYLATION

Another distinct hallmark of cancer is protein glycosylation since it is the most frequent posttranslational modification (PTM) and relatively half of all human proteins are glycosylated (Scott e Drake, 2019). The earliest evidence established that plant lectins show enhanced binding and agglutination of tumour cell. Later, *in vitro* cellular assays and *in vivo* animal studies have supported the conclusion that glycan changes are critical to several aspects of tumour cell behaviour (Varki A, Cummings RD, Esko JD, et al., 2022). Interestingly, ABC proteins related to the CDR phenotype are N-glycosylated glycoproteins.

Glycosylation is the enzymatic process responsible for the attachment of glycans to proteins, lipids, or other saccharides, which is catalysed by glycosyltransferases and glycosidase. These enzymes assemble monosaccharide moieties into linear and branched glycan chains (Rini JM, Moremen KW, Davis BG, et al., 2022). Therefore, there are multiple enzyme recognition sites in both secreted and membrane proteins, along with stereochemical α or β conjugations, that create further diversity in the attachment of these sugars. The assembly of both oligosaccharides and polysaccharides generates glycans that acquire heterogeneity and varying properties since diverse structures can be put together by simply linking different monosaccharides through glycosidic bonds (Reily *et al.*, 2019). Glycans can be categorized into three biological functions, such as (1) structural and modulatory features; (2) specific recognition by other molecules, as information carriers, generally glycan-binding proteins (GBPs); and (3) metabolism regulators (Gagneux P, Hennet T, Varki A., 2022).

In mammals the most common monosaccharides found in glycoconjugates all derive from glucose, that is, glucose (Glc), galactose (Gal), N-acetylglucosamine (GlcNAc), N-acetylgalactosamine (GalNAc), fucose (Fuc), mannose (Man), xylose (Xyl), glucuronic acid (GlcA), and sialic acid (Sia or Neu5Ac) (Figure 1.5).

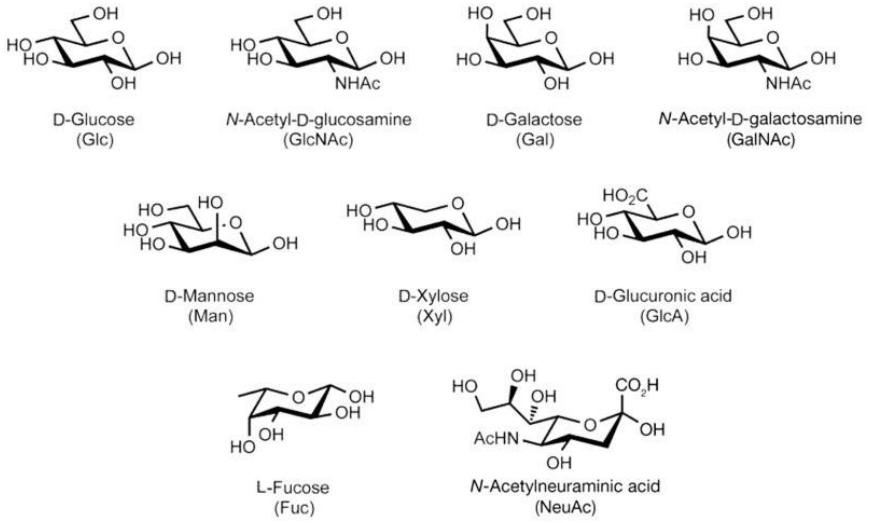


**Figure 1.5 -Common monosaccharides found in vertebrates.** N-Acetylneuraminic acid is the most common form of sialic acid. FROM: Seeberger PH, 2022.

Thus, glycans can have different functions in different tissues, at different times in development or in different environmental contexts, indicating that glycosylation is a site-specific modification (Gagneux P, Hennet T, Varki A., 2022). This allows them to regulate a diversity of biological processes, including protein folding, intracellular trafficking, cell-cell and cell-matrix interactions (glycocalyx interactions), cellular differentiation and immune responses (Lebrilla CB, Liu J, Widmalm G, et al., 2022).

### 1.3.1 TYPES OF GLYCOSYLATION

Branching is the prime characteristic of several glycans therefore glycan structures of glycoproteins are determined by the enzymatic transfer of sugar moieties. In eukaryotes, both membrane and secretory proteins pass through the endoplasmic reticulum (ER) and Golgi apparatus pathway, the compartment where major protein maturation occurs (Silsirivanit, 2019). Glycosylation is mediated by substrate availability, enzyme activity, levels of gene transcription and glycosyltransferases and glycosidases' location within the organelles (Reily *et al.*, 2019). Thus, a glycoprotein may have covalently attached one or more different glycans to its' polypeptide chain.

In humans, there are two main types of protein glycosylation: N-glycosylation and O-glycosylation. Nevertheless, the same protein can undergo more than one type of

glycosylation. This is based on the linkage of glycans to the amino acid residue, then N-linked glycans are attached to the nitrogen atom of an asparagine (Asn) residue side chain that is a part of the consensus peptide sequence Asn-X-Ser/Thr, where X represents any amino acid except proline (Pro). And O-linked glycans are attached to de oxygen atom of serine (Ser) or threonine (Thr) residues with functional hydroxyl groups (Reily *et al.*, 2019). Since there are two types of glycans, their biosynthesis is slightly distinct. O-glycosylation develops in the Golgi apparatus pathway of eukaryotic cells, in which O-glycans are structured and sugar residues are gradually added to the protein by several glycosyltransferases.

In N-glycosylation, the ER-Golgi pathway, glycans are previously structured in the cytoplasmic and lumen face of the ER membrane before being transferred “en bloc” to an Asn residue and are processed still in the ER lumen, succeeding within the Golgi following protein maturation modified by glycosyltransferases and glycosidases, that add and remove sugar residues, respectively (Figure 1.6).

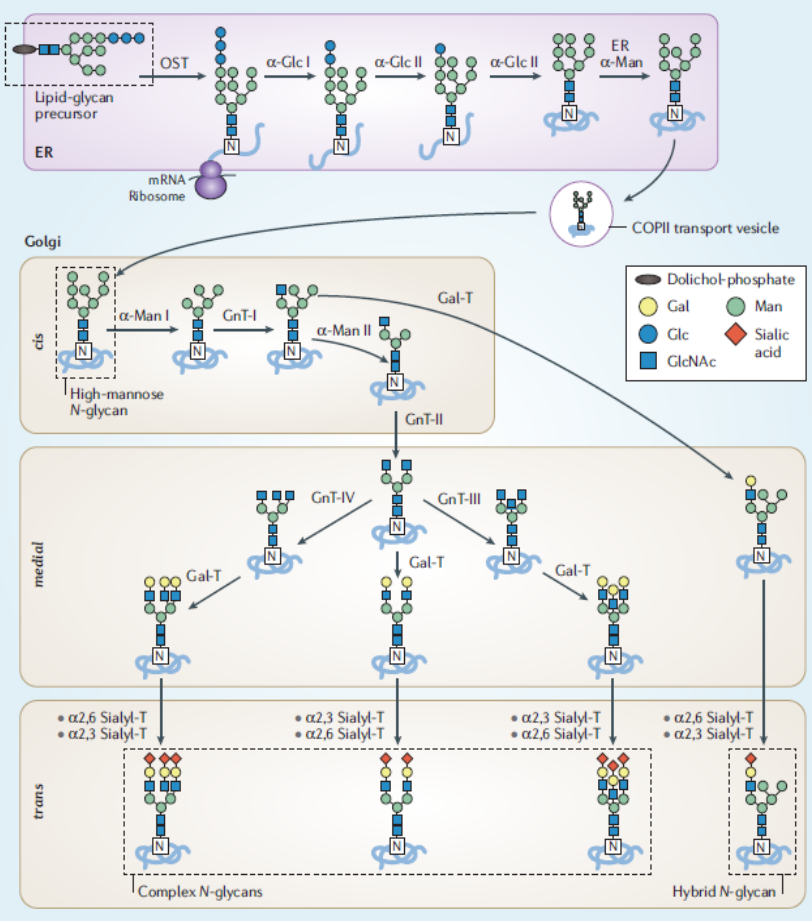


**Figure 1.6 - Processing and maturation of an N-glycan in the secretory pathway.** N-glycan synthesis initiates in the ER with the “en bloc” transfer of a lipid-glycan precursor (which is, Glc3Man9GlcNAc2 bound to dolichol phosphate) to Asp by oligosaccharyltransferase (OST). The glucose residues are sequentially removed by two α-glucosidases (α-Glc I–II) and an initial Man residue is removed by the ER α-mannosidase (α-Man). After a quality-control checkpoint, the glycoprotein proceeds to the Golgi apparatus for additional trimming by α-Man I–II and further glycan modifications. The final site affects the N-glycan composition through the expression levels of glycosyltransferases, the accessibility of the glycoprotein glycosylation sites and how long does the glycoprotein remains in the ER and Golgi apparatus. Source: Reily, C. *et al.*, 2019.

All N-glycans possess the same core sequence, comprising three mannose residues and two N-acetylglucosamine residues linked to an Asn:

Manα1-3(Manα1-6)Manβ1-4GlcNAcβ1–4GlcNAcβ1–Asn-X-Ser/Thr

However, there are three types of N-glycans defined on its branching residues, **(1)** Oligomannose, in which Man residues extend the core, **(2)** Complex, in which branches begin with GlcNAc residues and **(3)** Hybrid, in which one arm of the core is extended by Man residues and the other one by GlcNAc (Figure 1.7).

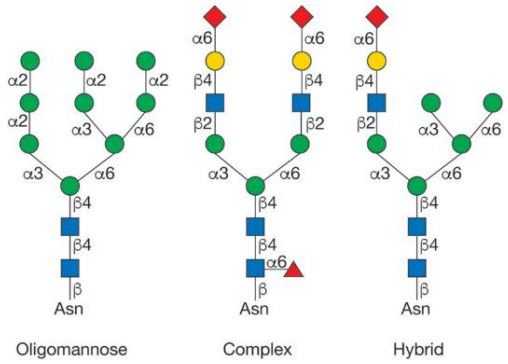


**Figure 1.7 – Three types of N-glycans: oligomannose, complex, and hybrid.** Each N-glycan contains the core Man3GlcNAc2Asn. From: Stanley P, Moremen KW, Lewis NE, et al., 2022.

In O-glycosylation, the initiating sugar residue linked to the oxygen atom in Ser/Thr is GalNAc. Consequently O-glycans, or O-GalNAc, are extended to form one of the four core sequences shown in Table 1.3 and Figure 1.8, designated Core 1 through 4, subsequently each glycan can be further extended or modified in a linear or branched O-glycan. Core 1 and 2 of O-glycans are commonly found in glycoproteins produced in many distinct cells (Brockhausen I, Wandall HH, Hagen KGT, et al., 2022).

**Table 1.3 - O-glycans cores 1 to 4**. Addapted from: Brockhausen I, Wandall HH, Hagen KGT, et al., 2022.

| | |
|---|---|
| **Core 1** | Galβ1-3GalNAcαSer/Thr |
| **Core 2** | GlcNAcβ1-6(Galβ1-3)GalNAcαSer/Thr |
| **Core 3** | GlcNAcβ1-3GalNAcαSer/Thr |
| **Core 4** | GlcNAcβ1-6(GlcNAcβ1-3)GalNAcαSer/Thr |

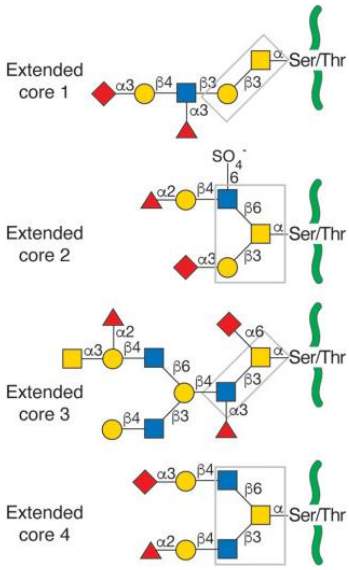


**Figure 1.8 - O-glycans cores structures 1 to 4.** Green lines are protein. Addapted from: Brockhausen I, Wandall HH, Hagen KGT, et al., 2022.

The mature glycan extensions of both N-glycans and O-glycans, meaning their terminal/peripheral sugars, often regulate the functions or recognition properties of glycoproteins. This elongation or "capping" takes place at the end of the pathway, in the *trans*-Golgi network (TGN), after the O-glycans, hybrid and complex N-glycans are assembled.

The most important added sugars are sialic acid (Sia) and fucose (Fuc), through sialylation and fucosylation, respectively, given that its' developed antigens impact on several functions in the cell. For instance, core fucosylation leads to the biosynthesis of Lewis antigens that are known to mediate adhesion between tumour cells, the addition of α1-3Fuc or α1-4Fuc to the Asn-linked GlcNAc in the N-glycan core results in Lewis X ($Le^x$) or Lewis A ($Le^a$) antigens, correspondingly (Figure 1.9). Other Lewis antigens prominent in various cancers and used as tumour biomarkers are Sialyl Lewis X ($sLe^x$) and Sialyl Lewis A ($sLe^a$), these are further sialylated, by addition of α2-3Sia linkage to the Gal sugar (Figure 1.9). Recently, $sLe^x$ has been proposed as a marker for monitoring the metastatic progression of BC (Ma *et al.*, 2021). Another sialylated antigen is Sialyl Thomsen-nouveau (sTn) that results from the addition of a α2-6Sia to a core 1 O-glycan (Neu5Acα2-6GalNAcα-

O-Ser/Thr). Increased sTn is associated with invasiveness and metastatic properties in tumour cells as well as resistance to chemotherapy (Eavarone *et al.*, 2018).

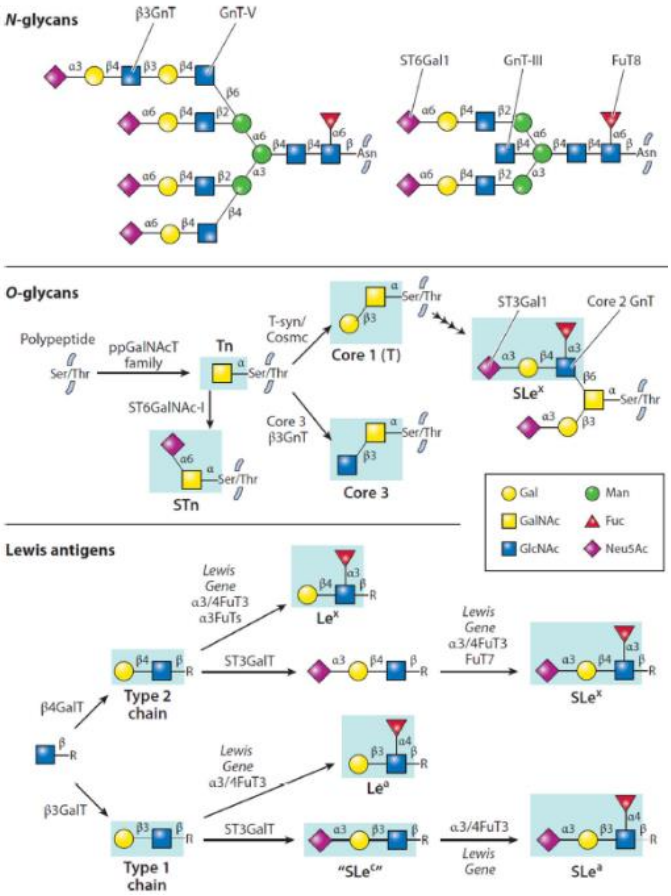


**Figure 1.9 – Specific structures of N- and O-glycans and Lewis antigens with the enzymes responsible for the addition of specific sugar residues**. Antigens indicated in blue boxes represent the major determinants recognized by monoclonal antibodies. T antigen: Core 1 disaccharide (Galβ1-3GalNAc); Tn (Thomsen-nouveau) antigen: GalNAcα-O-Ser/Thr; STn (Sialyl Thomsen-nouveau) antigen: Neu5Acα2-6GalNAcα-O-Ser/Thr; $Le^x$ (Lewis X) antigen: Galβ1-4(Fucα1-3)GlcNAcβ-R; $SLe^x$ (Sialyl Lewis X) antigen: Neu5Acα2-3Galβ1-4(Fucα1-3)GlcNAcβ-R; $Le^a$ (Lewis A) antigen: Galβ1-3(Fucα1-4)GlcNAcβ-R; $SLe^a$ (Sialyl Lewis A) antigen: Neu5Acα2-3Galβ1-3(Fucα1-4)GlcNAcβ-R. Source: Stowell *et al.* (2015).

## 1.4 GLYCOSYLATION IN CANCER

Glycosylation is a highly sensitive process to the physiological state of the cell and several studies have verified distinct modifications of this process in human diseases, particularly, in cancer, which are often related to the beginning of the EMT. For example, during the invasion and metastasis of BC cells, epidermal growth factor receptor (EGFR), HER2 and transforming growth factor-β (TGF-β) receptor are abnormally glycosylated (Liu *et al.*, 2020; Reily *et al.*, 2019). As indicated before, cancer induces the abnormal increase in cell proliferation and alters its genome and, consequently, its glycome, changing the cellular glycosylation patterns. Cell surface glycans comprise a major part of the membrane, which is designated as glycocalyx, i.e., the dense meshwork of glycoproteins, glycolipids and glycosaminoglycans attached to membrane proteins, lipids and extracellular matrix (ECM) proteins (Scott e Drake, 2019). Since cells exhibit altered glycosylation patterns in cancer and glycans impact in cells' functions and interactions, these modifications can end up favouring pathogenic tumour development, progression, metastasis, cell adhesion, cell-ECM interactions, cellular signalling, and glycoprotein folding in tumour cells (Silsirivanit, 2019). Thus, protein glycosylation is a hallmark of cancer and a relevant biomarker as these modifications are not a random consequence of disordered biosynthesis in tumour cells, glycans are rather selected to regulate tumour proliferation, invasion, metastasis and angiogenesis (Munkley e Elliott, 2016).

Glycan changes in tumour cells vary from loss or excessive expression of specific glycans, increased expression of truncated glycans, sialylation, fucosylation and, less frequently, the appearance of neo-synthesized glycans (Bellis SL, Reis CA, Varki A, et al., 2022). The main impaired types of glycosylation are N-glycans and O-glycans (O-glycan truncation is most common) and these modifications may occur both early and late in cancer progression and metastasis (Figure 1.10). Usually they are characterized by specific alterations in N- and O-glycan core structures and further branching (mainly N-glycan branching), generating different terminal glycan motifs, which modifies overall glycan structure and function (Wang *et al.*, 2015).

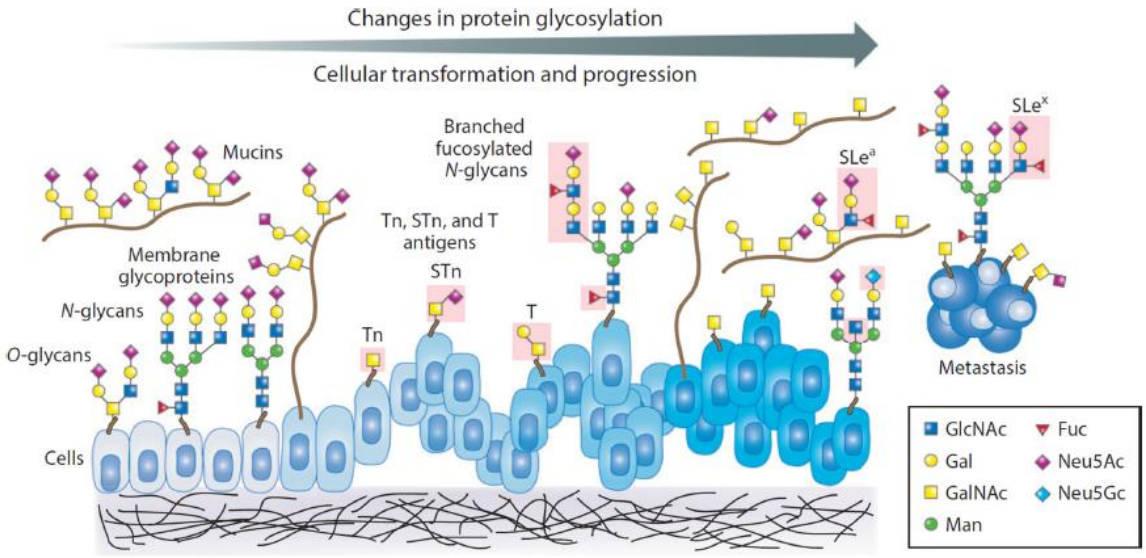


**Figure 1.10 - Changes in protein glycosylation on membrane and soluble glycoproteins during cellular cancer progression and transformation.** Red-boxed areas highlight changes in O-glycans (T, Tn, and sTn antigens) and in N-glycans ($sLe^x$ and $sLe^a$). Source: Stowell et al. (2015).

However, these altered glycosylation patterns found in cancer have been denominated 'oncofetal' as they resemble patterns often seen in early development. This includes truncated glycosylation, which is associated with decreased cell adhesion, increased tumour growth and cell migration, invasion and poor prognosis (Pinho e Reis, 2015). Truncated O-Glycans, such as Tn antigen (GalNAc-Ser/Thr), T antigen (Gal-GalNAc-Ser/Thr), and sTn (Figure 1.11), often appear in the bloodstream and were identified as pan-carcinoma biomarkers in breast, colon, oesophageal, pancreatic and gastric cancer (Silsirivanit, 2019).

Another oncofetal pattern is neo-synthesis, which comprises modifications such as abnormal core fucosylation, *N*-glycan branching - the degree of branching modulates the activity and signalling of growth factor receptors (Munkley e Elliott, 2016)- and an overall increase in cell-surface Sia (Reily *et al.*, 2019). In BC the most recurrent alterations in glycosylation patterns are shortened O-glycans and increased sialylation (Andergassen *et al.*, 2015).

Sialylated glycans are decisive in cellular recognition, cell adhesion and signalling, hence an increase in α2,6- and α2,3-linked Sia has been related to neoplasia. This rise leads to a physical disruption in cell-cell adhesion, promoting the detachment from the tumour mass and then the invasion of the surrounding tissue (Munkley e Elliott, 2016). Lewis' antigens, such as $sLe^x$ and $sLe^a$ (CA 19-9), are sialylated glycans highly expressed in a

considerable number of cancers (Figure 1.11). $SLe^x$ antigen interacts with selectins which end up regulating the metastatic cascade and determining the malignant behaviour and development of metastasis. Therefore, $sLe^x$ relates to poor survival in BC patients. And the $sLe^a$ antigen is detected by the serological assay CA 19-9, this glycan is considered a biomarker in cancer, and is used to monitor clinical response to therapy (Pinho e Reis, 2015). Tumour cells also resort to their glycosylation mechanisms to modify glycans on cell death receptors, enabling them to resist apoptosis. Thus, these altered glycoforms directly impact the metastatic potential of this disease (Khosrowabadi *et al.*, 2022).

In each of these situations, the glycans present on a given glycoprotein are dictated in part by the expression, localization, and activity of the glycosyltransferases in a given cell (Wang *et al.*, 2015).

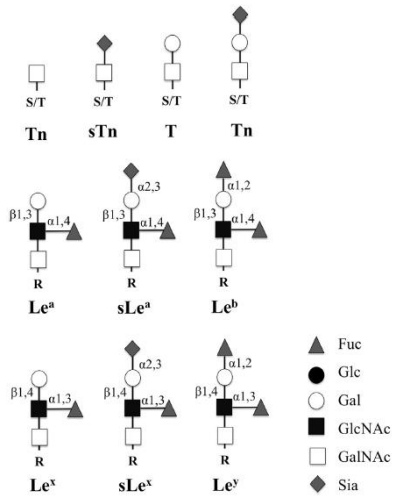


**Figure 1.11 - Some cancer associated glycan biomarkers**. Source: Silsirivanit A. (2019).

## 1.5 GLYCOME AND CHEMORESISTANCE IN BC

Thus, one prime transformation process of a normal cell into a malignant cell is determined by a change in its' glycome, which can negatively impact glycan modifications in several ways and thus the biological activity of a cell. The Cancer Genome Atlas (TCGA) has verified multiple changes in glycosylation gene expression that are related to cancer (Bellis SL, Reis CA, Varki A, et al., 2022). Over 200 gene-encoded enzymes are known to interfere in glycosylation concise pathway (Wang *et al.*, 2015). As mentioned, protein glycosylation is regulated by innumerous mechanisms that involve the expression and localization of glycosyltransferases and glycosidases in the ER-Golgi pathway and the concentration and availability of nucleotide sugar donors and transporters. This is due to dysregulation during DNA transcription, dysregulation of related proteins, such as chaperones, and/or through altered enzyme activity responsible for glycosylation (Scott e Drake, 2019; Silsirivanit, 2019).

CDR has been proven to be related with altered glycosylation patterns since various glycoproteins can be overexpressed and aberrantly glycosylated in cancer resistance, which regulates not only cell survival and growth, but also tumour immunomodulation and consequent metastasis. For example, it was demonstrated that in tumour cells N-glycans inhibit programmed cell death ligand 1 (PD-L1) antibody recognition, which demonstrates that therapeutic antibodies are unsuccessful in binding to certain PD-L1 glycoforms (Costa *et al.*, 2020). On the other hand, glycosyltransferases expression is regulated through both transcription factors and epigenetic mechanism that are certainly linked to CDR (Diniz *et al.*, 2022; Fonseca, da *et al.*, 2016).

The transport and corresponding glycosylation of glycoproteins through the ER-Golgi pathway is highly efficient and specific, considering each enzyme has specific requirements for its location in the membranes of these organelles and that every glycosyltransferase is near a nucleotide sugar transporter with similar substrate specificity. These proteins are categorized in different subfamilies regarding the respective transferred carbohydrate and misregulation of these sugar transporters affects sugar concentration and consequently the glycosylation pattern of each cell. For instance, enzymes involved in the beginning of glycosylation are located in the *cis* and *medial* Golgi and those in the latter steps of the pathway are in the *trans* Golgi and TGN (Silsirivanit, 2019).

Importantly, ABC transporters (ABCB1, ABCC1 and ABCG2 related to CDR in BC) undergo N-glycosylation, the human ABCB1 glycoprotein only has three out of the ten consensus sequences glycosylated (N91, N94 and N99). In 1995, Kramer et al. observed that tunicamycin supressed this transporter activity as cytostatic drugs accumulated into the cells – tunicamycin is an active drug against BC which inhibits GlcNAc transfer to dolichol phosphate in the ER, blocking N-glycosylation therefore disrupting protein maturation (Fonseca, da *et al.*, 2016; Liu *et al.*, 2020).

Moreover, downregulation of certain genes through DNA methylation or histone deacetylation/trimethylation may supress glycosylation genes that restrain tumour progression, as cells with EMT phenotype downregulate *MGAT3*, while upregulating *MGAT5* and *ST6GAL1* (Bellis SL, Reis CA, Varki A, et al., 2022). These indispensable glycotransferases and glycosidases directly influence the structure of glycans impacting cancer progression and metastasis, consequently, cancer cells become chemoresistant, thus some of them may be considered as biomarkers (Table 1.4).

**Table 1.4 - Enzymes associated with aberrant glycosylation as cancer biomarkers**. Adapted from: Meany *et al*., 2011; Huimin *et al*., 2020; Fonseca *et al*., 2016; Aurélie *et al*., 2010)

| Enzyme | Implication in aberrant glycosylation |
|---|---|
| 4-Beta-N-Acetylglucosaminyltransferase (MGAT) | Increase cell migration and metastasis |
| Polypeptide N-Acetylgalactosaminyltransferase 6 (ppGALNAc-T) | Increase incomplete synthesis of O-glycans |
| N-Acetylglucosaminyltransferase V (GlcNAcT-V) | Increase β1-6 branching of N-glycans |
| α2,3-Sialyltransferase | Increase sialylated glycans and reduce cell adhesion, promoting tumorigenisis |
| α2,6-Sialyltransferase | |
| α1,2-Fucosyltransferase | Reduce cell adhesion, promoting metastasis and invasion |
| α1,3-Fucosyltransferase | |
| α1,4-Fucosyltransferase | |

Additionally, increased glycans with added Sia, which occurs via sialyltransferases upregulation, promotes tumour metastasis. ST6GalNAc-I is the glycosyltransferases responsible for the sialylation of the Tn antigen, generating the sTn antigen, which is abnormally distributed across the Golgi cisternae increasing the number of immature O-glycans (Diniz *et al.*, 2022). In MDA-MB-231 BC cells, this glycan is detected at high levels, enhancing the tumorigenicity of these cells (Meany e Chan, 2011). In contrast, another sialyltransferase is ST6GalNAc2, identified as a metastasis suppressor in BC cells which is linked to patient survival (Munkley e Elliott, 2016; Silsirivanit, 2019; Wang *et al.*, 2015).

Multiple other enzymes can also intervene in O-glycans truncation, such as polypeptide GalNAc transferases (ppGalNAcTs) which are the enzymes responsible for the first step in O-glycosylation (including the development of Tn antigen), e.g., GALNT6 stands out dysregulated in BC, it is believed that the overexpression of this gene may contribute to mammary carcinogenesis through aberrant glycosylation and stabilization of MUC1, contributing to chemoresistance. Further, overexpression of *MGAT5* in MCF-7 cells increases resistance to PAX and other chemotherapeutics (doxorubicin and vincristine). This enzyme is essential for the synthesis of hybrid and complex N-glycans (Fonseca, da *et al.*, 2016).

Another group of enzymes, fucosyltransferases (FUTs), are responsible for the fucosylation of sugar chains and currently 13 different FUTs have been identified. It was demonstrated that this PTM is associated with CDR and metastatic potential in BC since the upregulation of FUT-encoding genes and, ergo, the presence of Fuc influences growth factor receptor activation and signalling, cell-cell/ECM adhesion receptors and immune checkpoint inhibitors. For example, FUT8 promoted the TGF-β signalling pathway, enhanced the migration and invasion of BC cells, and potentially promoted their distant metastasis to the lungs (Liu *et al.*, 2020; Schjoldager *et al.*, 2020).

Overall, tumour cells display several noticeable modifications in their glycome, developing functional consequences for cancer pathogenesis and aggregating a plethora of data that correlates aberrant glycosylation during cancer development with drug resistance. Considerable glycosylation changes commonly appear however, the specific molecular mechanism is still unclear.

## 2. AIMS

The main goal of this project is to assess differential protein glycosylation in BC cells, to analyse altered glycosylation patterns in BC cells, as they develop resistance to PAX and to understand whether glycosylation is a critical feature of PAX resistance.

To achieve this, a breast cell line resistant to PAX (MDA-MB-231/PAX) was previously established, by exposing cells to increasing concentrations of the drug. Protein extracts were prepared to assess protein glycosylation in PAX-sensitive and PAX-resistant cells through western blot, using different antibodies. Real-time PCR (RT-PCR) assays were used to evaluate modifications on the glycosylation genes expression level and to correlate with resistance, at different PAX concentrations.

# 3. METHODS AND MATERIALS

## 3.1 Cell Culture

In this project, we used a human breast adenocarcinoma cell line – MDA-MB-231. This epithelial cell line is a TNBC which is highly aggressive, invasive and poorly differentiated and is deficient in ER, PR as well as HER2 expression. The MDA-MB-231 cell line was provided by Professor Nuno Oliveira from Faculdade de Farmácia from Universidade de Lisboa and the MDA-MB-231 cell line resistant to PAX (MDA-MB-231/PAX) established previously by our group (Duarte, C. 2022). Cells were cultured in Dulbecco's Modified Eagle's Medium (DMEM)-low glucose (Sigma-Aldrich, #D6046-500ML) supplemented with 10% Fetal Bovine Serum (FBS) (Sigma-Aldrich, #F7524) and 1% of Penicillin-streptomycin (Sigma-Aldrich, #P4333) at 37°C in a humidified 5% $CO_2$ incubator. The culture conditions of the parental cell line (untreated control, PAX-sensitive) and MDA-MB-231/PAX cells were identical, except that in MDA-MB-231/PAX there was exposure to the drug in different PAX concentrations (400nM, 800nM and 1000nM). The intended concentrations to cell culture (400nM and 1000nM) were obtained through the dilution of the PAX stock solution (Cytoskeleton Inc., #TXD01) which has a concentration of 2mM after reconstitution.

Meanwhile when cells reached a confluence of approximately 80%, they were sub-cultured through trypsinization. To sum up, cells were detached from the T-flasks (SARSTEDT) by first washing with versene (EDTA solution in PBS) plus sodium bicarbonate (Sigma-Aldrich, #4549) and then by adding a solution of trypsin diluted in versene (1:10) plus sodium bicarbonate. Subsequently, medium was added to halt trypsin activity and cell suspension was centrifuged at 1000rpm for 5 minutes at room temperature (RT). The pellet was resuspended in medium and afterwards subcultured into a new flask.

## 3.2 Protein Glycosylation analysis

### 3.2.1 Protein extraction

Membrane and cytoplasmic protein fractions were isolated using Mem-PER$_{TM}$ Plus Membrane Protein Extraction Kit according to the manufacturer's instructions (Thermo-Fisher, #89842Y).

Briefly, cells were resuspended in medium and centrifuged at 300 x g for 5 minutes. After washing the cell pellet with 3 mL of Cell Wash Solution, cells were centrifuged again in the same conditions. The resultant pellet was resuspended in 1,5 mL of Cell Wash Solution and transferred to a 2 mL tube to be centrifuged at 300 x g for 5 minutes. Then the supernatant was discarded and 0,75 mL of Permeabilization Buffer was added to the cell pellet and the solution was vortexed briefly to obtain a homogeneous cell suspension, followed by incubation for 10 minutes at 4°C with constant mixing. Following the centrifugation of the cell suspension at 16000 x g for 15 minutes, the resultant supernatant contained the cytosolic proteins which was carefully removed and transferred to a new tube. The pellet was resuspended in 0,5 mL of Solubilization Buffer, and the tubes were incubated at 4°C for 30 minutes with constant mixing. Next, tubes were centrifuged at 16000 x g for 15 minutes at 4°C and the supernatants containing membrane and membrane-associated proteins were transferred to new tubes. The cytosolic and membrane proteins were stored at -80°C until further use.

### 3.2.2 Protein Quantification

Protein quantification was executed through the Bradford Assay. This method is an easy and quick technique that allows to determine protein concentration and is also recommended for assessing protein concentrations for gel electrophoresis. This process is found on the absorbance shift of Coomassie Brilliant Blue G-250 (Coomassie Blue) dye when binding to proteins in solution, when this happens the red form of the dye is converted into its blue form and the $Abs_{max}$ is 595 nm.

The assay uses standards to both quantify protein and to subtract any background. The calibration curve was assembled using Bovine Serum Albumin (BSA) stock solution of 2 mg/mL (Bio-Rad, #500-0206) at different concentrations (0, 0,002, 0,004, 0,008, 0,016, 0,032, 0,064 and 0,128µg/µL). Membrane protein samples of MDA-MB-231 parental and resistant cell line (400nM and 1000nM) were diluted in distilled water (1:250) and 200µL of Bradford reagent (Bio-Rad, #500-0006) was formerly added to each dilution of BSA and protein sample. These samples triplicates were transferred to a 96-well microplate and after 15 minutes of incubation at RT, the absorbance was read at 595 nm (SpectraMax i3x plate reader, Molecular Devices).

### 3.2.3 Glycoprotein glycosylation Pattern

In order to have a broad analysis of the glycosylation pattern we used the Pierce™ Glycoprotein Staining Kit (Thermo Fisher, #24562). This is a fast and sensitive colorimetric kit, it is used to detect glycosylated proteins in polyacrylamide gels or nitrocellulose membranes using the periodic acid-Schiff (PAS) method. This method detects polysaccharides, such as glycoproteins since when they are treated with periodic acid, glycols present in sugars are oxidized to aldehydes, these then react with the Schiff reagent yielding magenta colour bands.

This kit was performed in Sodium Dodecyl Sulfate-Polyacrylamide Gel Electrophoresis (SDS-PAGE) to separate proteins by their molecular weight, gels and samples were prepared and loaded as in western blot analysis.

#### 3.2.3.1 Sample preparation

After determining protein concentration through the Bradford method and reconstituted the positive and negative controls, each well was loaded with 6µg of protein. Protein samples were then denatured in 2x Loading Buffer (10% SDS, 50% Glycerol, 1 M Tris-HCL pH 6.8, 1% Bromophenol Blue, and ddH2O) plus 10% of β-mercaptoethanol in a 1:1 ratio and heated in for 8 minutes at 100°C.

#### 3.2.3.2 Electrophoresis and Glycoprotein Staining

Samples were loaded in 4% stacking and 8% resolving gel (Table 7.1, in Annex 1) for glycosylation analysis and the electrophoresis was performed in Running buffer 1X (stock solution 5X: 0.1% SDS; 25 Mm Trizma-base; 250 mM Glycine; pH 8.3) at 100 V for 90 minutes. Staining reagents are in Table 7.2 in Annex 1.

The following steps were performed in a fume hood. The gel was completely immersed in 100 mL of 50% methanol and fix for 30 minutes and after washed in 100 mL of 3% acetic acid with gently agitation for 10 minutes, twice. Next, gel was incubated with 25 mL of Oxidizing Solution with gentle agitation for 15 minutes. Then the gel was washed three times with 100 mL of 3% acetic acid for 5 minutes. Following another incubation with 25 mL of Glycoprotein Stain with gentle agitation for 15 minutes, to be subsequently transferred to 25 mL of Reducing Solution for 5 minutes with agitation. In the last step, the gel is washed with 3% acetic acid and then with ultrapure water. Glycoproteins appear as magenta bands. The polyacrylamide gel was stored in acetic acid.

### 3.2.4 Western Blot

Western Blot is a technique used to detect proteins of interest, however, in this particular case, we intended to analyse glycosylation patters in membrane proteins. This method involves Sodium Dodecyl Sulfate-Polyacrylamide Gel Electrophoresis (SDS-PAGE) to separate proteins by their molecular weight, that are afterwards transferred to a nitrocellulose of polyvinylidene fluoride (PVDF) membrane. Next, specific glycans in glycoproteins are highlighted using a primary antibody and then a secondary antibody conjugated with labelled chemiluminescent or fluorescent molecule, which allows us to detect the antigen-antibody binding signal.

#### **3.2.4.1** Sample preparation

After determining protein concentration through the Bradford method and the amount of protein in each well (20µg), protein samples were denatured in 2x Loading Buffer (10% SDS, 50% Glycerol, 1 M Tris-HCL pH 6.8, 1% Bromophenol Blue, and ddH2O) plus 10% of β-mercaptoethanol in a 1:1 ratio and heated in for 8 minutes at 100°C.

#### **3.2.4.2** Electrophoresis and Western Blot

Samples were loaded in 4% stacking and 8% resolving gel (Table 7.1, in Annex 1) for glycosylation analysis and the electrophoresis was performed in Running buffer at 100 V for 90 minutes. The separated proteins were transferred into a PVDF membrane at 100 V for 1 hour with a refrigerated unit using Transfer buffer 1X (stock solution 5X: 0.04% SDS; 48 mM Trizma-base; 39 mM Glycine; 10% methanol; pH 8.3). Then, membranes were washed twice for 5 min with MilliQ water, blocked with Blocking Buffer from WesternDot™ 625 Goat Anti-Mouse Western Blot Kit (Thermo Fisher, Invitrogen, # W10132) for 1h under agitation at RT and after incubated overnight with the primary antibody, at 4°C, diluted 1:1000 ratio in Wash Buffer 1X. Later, PVDF membranes were washed three times for 5min with Wash Buffer 1X, followed by 1h incubation with the secondary antibody (Biotin-XX goat anti-mouse IgG (H+L), Invitrogen #W10132 C) diluted 1:1000 ratio in Wash Buffer 1X, at RT. Membranes were washed again, to be incubated with streptavidin conjugate (Qdot™ 625, Invitrogen #W10132 D) diluted 1:2000 ratio, for 1h at RT, followed by another washing with Wash Buffer 1X.

Immunoreactivity of the membranes was detected by using the ChemiDoc Touch Imaging System (Blot Qdot 625 filter, Bio-Rad). The pictures acquired were then inverted and the band were relatively quantified through the Image Lab software.

Spectra™ Multicolor Broad Range Protein Ladder (Thermo Fisher, #26634) and PageRuler™ Plus Prestained Protein Ladder (Thermo Fisher, #26619), 10 to 260 kDa and 10 to 250 kDa, respectively, were used as protein molecular markers.

The primary antibodies (Table 3.1) used were mouse anti-Le X (R&D, # IC2155T-050UG), mouse monoclonal anti-O-GlcNAc (Santa Cruz, #sc-59623), mouse anti-sLe A (Santa Cruz, #sc-59480), mouse anti-sLe X (Millipore, #2096) and mouse monoclonal anti-HNK-1 (Sigma, #C0678).

**Table 3.1 – Mouse monoclonal antibodies and its specificity.** Provided by Professora Júlia Costa, Glycobiology Lab, ITQB | Universidade NOVA de Lisboa

| Antibody | Detects |
|---|---|
| Anti-O-GlcNAc | Ser-O-GlcNAc and Thr-O-GlcNAc |
| Anti-HNK-1 | HSO3-3GlcAβ1-3Galβ1-4GlcNAc-R |
| Anti-Le X | Galβ1-4(Fucα1,3)GlcNAc-R |
| Anti-sLe X | Siaα2,3Galβ1,4(Fucα1,3)GlcNAc-R |
| Anti-sLe A | Siaα2,3Galβ1,3(Fucα1,4)GlcNAc-R |

### 3.2.5 Real Time PCR analysis

#### 3.2.5.1 RNA Extraction

Total RNA was extracted from cells following the Direct-zol™ RNA Miniprep Plus kit (Zymo Research, #R2070) according to the manufacturer's instructions. As in protein extraction, cells were acquired through trypsinization and then resuspended in PBS to be centrifuged at 800 x g. After discarding de supernatant, cells were resuspended in 700 µL of Quiazol (Qiagen, #5346994), transferred to a 1,5 mL tube, vortexed and stored at -80°C.

After defrosting samples were vortexed for 2 minutes and centrifuged at 16000 x g for 30 seconds, to homogenate and remove any debris, respectively. The resultant supernatant was transferred into a new tube and the same volume of ethanol (95-100%)

was added to the supernatant and mixed thoroughly. This mixture was transferred into a Zymo-Spin™ IIICG Column in a Collection Tube and then centrifuged. The column was transferred into a new collection tube and the flow-through was discarded. To perform the DNase I treatment, 400 µL of RNA Wash Buffer was added to the column and centrifuged. Next, 5 µL DNase I and 75 µL DNA Digestion Buffer were added in a new tube and mixed by gentle inversion. This solution was directly added to the column matrix and incubated at RT for 15 minutes. After, 400 µL of Direct-zol™ RNA PreWash was added to the column and centrifuged and the flow-through was discarded, this step was performed twice. Next, was added 700 µL of RNA Wash Buffer to the column and centrifuged for 1 minute to ensure complete removal of the wash buffer. The column was the transferred carefully into a RNase-free tube. To conclude, 100 µL of DNase/RNase-Free Water was directly added to the column matrix and centrifuged to elute RNA. Samples were then stored at –80°C.

#### **3.2.5.2** RNA Quantification

RNA samples were quantified by measuring the amount of RNA in 1 µL of the required samples, using the Nanodrop 2000 spectrophotometer (Thermo-Fisher). For RT-PCR analysis, samples must have an equal or superior value to 1,9 in both A260/280 an A260/230 ratio.

#### **3.2.5.3** cDNA synthesis and RT-PCR

The RNA was converted into cDNA using the High-Capacity RNA-to-cDNA Kit (Applied Biosystems, #4387406), according to the manufacturer's instructions. We used 2 µg of total RNA per 20 µL reaction and prepared +RT reactions (containing the RNA sample and the enzyme) for the parental cell line and the resistant cell line (1000nM). The reactions were performed under the programmed thermal cycling conditions, incubated at 37°C for 1 hour, then heated at 95°C for 5 min and held at 4°C, using a the GeneAmp® PCR System 9700 thermocycler. cDNA was short-term stored at 4°C.

Real-Time PCR was performed using the TaqMan™ Array 96 - Well FAST Plate, Human Glycosylation (Applied Biosystems, #4413255) and the relative expression of the targeted genes and all the endogenous controls were measured through the TaqMan®

Gene Expression Assays (Applied Biosystems, #4427562) (Table 1). All these reactions were done in triplicates. Plate layout for each target in showed in Annex 2.

**Table 3.2 - Target and endogenous gene analysed through RT-PCR.**

| TARGET GENE | | | | ENDOGENOUS GENE |
|---|---|---|---|---|
| A4GNT | GALNT11 | HEXB | NEU2 | GAPDH |
| AGA | GALNT12 | B2M | NEU3 | HPRT1 |
| B3GLCT | GALNT13 | HBMS | NEU4 | GUSB |
| B3GNT2 | GALNT14 | MAN1A1 | OGT | ACTB |
| B3GNT3 | GALNT2 | MAN1A2 | POFUT1 | B2M |
| B3GNT4 | GALNT3 | MAN1B1 | POFUT2 | HBMS |
| B3GNT8 | POC1B-GALNT4,GALNT4 | MAN1C1 | POMGNT1 | IPO8 |
| B4GALT1 | GALNT6 | MAN2A1 | POMT1 | PGK1 |
| B4GALT2 | GALNT7 | MAN2A2 | POMT2 | RPLP0 |
| B4GALT3 | GALNT8 | MAN2B1 | PRKCSH | TBP |
| B4GALT5 | GALNT9 | MANBA | ST3GAL1 | TFRC |
| CIGALT1 | GALNT16 | MGAT1 | ST3GAL2 | |
| CIGALT1C1 | GALNTL5 | MGAT2 | ST6GAL1 | |
| EDEM1 | GALNTL6 | MGAT3 | ST6GALNAC1 | |
| EDEM2 | GANAB | MGAT4A | ST8SIA2 | |
| EDEM3 | GCNT1 | MGAT4B | ST8SIA3 | |
| FUCA1 | GCNT3 | MGAT4C | ST8SIA4 | |
| FUCA2 | GCNT4 | MGAT5 | ST8SIA6 | |
| FUT11 | GLB1 | MGAT5B | UGGT1 | |
| FUT8 | GNPTAB | MOGS | UGGT2 | |
| GALNT1 | GNPTG | NAGPA | 18S | |
| GALNT10 | HEXA | NEU1 | | |

Preparing the plate, each reaction was reconstituted following the protocol provided by the manufacturer, applying TaqMan® Fast Universal PCR Master Mix, no AmpErase™ UNG and cDNA samples were diluted in nuclease-free water, to contain 20 ng per 10 µL reaction. The cDNA-Master Mix mixture was transferred to each well and, after homogenization and centrifugation, was transferred again to a MicroAmp® Optical 96-Well Reaction Plate (Applied Biosystems, #N8010560). Succeding importing the setup file into the QuantStudio™ 5 RT-PCR Instrument (Applied Biosystems, #A28134), we

selected the appropriate thermal protocol: UNG incubation at 50°C for 2 min, enzyme activation at 95°C for 20 sec, followed by 40 cycles at 95°C for 1 sec and at 60°C for 20 sec.

The expression level of the targeted genes was determined from the obtained $C_t$ values. $\Delta C_t$ was calculated through the subtraction of the $C_t$ of each target gene with the avegared $C_t$ of all the endogenous controls ($\Delta C_t$ = $C_t$ (target gene) – $C_t$ (average of endogenous controls)). These values were then used to determine the relative expression between PAX-sensitive cells and the PAX-resistant cells (1000nM) by calculating $2^{-\Delta\Delta Ct}$ of every target gene ($\Delta\Delta C_t$ = $\Delta C_t$(MDA-MB-231/PAX target gene) - $\Delta C_t$(MDA-MB-231 target gene)).

#### 3.2.5.4 Statistical analysis

We analysed our data with GraphPad Prism 9 software. In the expression assay, values were presented with an approximate mean ± standard error of the mean (SEM), and the statistical analysis was performed by applying a Mixed-effects model (REML) with Dunnett's multiple comparison test. A p-value<0.005 was considered statistically significant in these assays.

# 4. RESULTS

## 4.1 PROTEIN GLYCOSYLATION PATTERN ANALYSIS

Initially, the Pierce™ Glycoprotein Staining Kit (Thermo Fisher, #24562) was used to assess differential protein glycosylation between the parental PAX-sensitive cells and the resistant cells. Unfortunately, the sensitivity of the kit was not enough to detect glycosylated proteins in any sample, despite all the optimizations made to the protocol. First, the concentration of samples was increased and then, both sample concentration and incubation time with the oxidation agent were increased, to make sure all glycoproteins were oxidized. Nevertheless, the kit did not detect any glycosylated proteins, for reasons unknown.

In order to understand whether there are considerable differences in protein glycosylation between PAX-sensitive (MDA-MB-231) and Pax-resistant cells (MDA-MB-231/400nM and MDA-MB-231/1000nM), we submitted the extracted membrane proteins to the western-blot technique. The protein samples were stained with five different mouse monoclonal antibodies (mAbs), anti-O-GlcNAC, anti-HNK-1, anti-Le X, anti-sLe X and anti-sLe A, in Table 4.1 and Figure 4.1, Figure 4.2, Figure 4.3, Figure 4.4 and Figure 4.5, respectively.

O-GlcNAc transferase (OGT) catalyses the addition of GlcNAC to specific Ser or Thr residues to form a β-glycosidic bond and does not form complex glycan structures. O-GlcNacylation (attachment of O-GlcNAc) is an unusual dynamic protein modification abundant within the nucleus and cytoplasm of eukaryotic cells. Proteins linked to aberrant O-GlcNAc play a key role in pathogenesis of tumours, studies imply that it stimulates invasion, metastasis, recurrence, and prognosis of BC (Lu *et al.*, 2022).

The HNK-1 (Human Natural Killer-1) epitope is an N-linked carbohydrate, recognized by the mAb HNK-1, is required for the structural and functional development of the mammalian nervous system. This sulphated carbohydrate is carried by limited number of molecules such as cell adhesion molecules, extracellular matrix proteins and glycolipids, which end up influencing malignant tumours invasiveness (Morita *et al.*, 2008; Nakagawa *et al.*, 2012).

Lewis antigens are known to mediate the proliferative, invasive, and metastatic capacity of tumour cells. $Le^x$, $sLe^x$ and $sLe^a$ are core fucosylated carbohydrate antigens, further addition of Sia to these epitopes originates more complex glycan structures ($sLe^x$

and sLe[a]). All these fucosylated epitopes are correlated with poor prognosis in TNBC patients (Blanas *et al.*, 2018; Koh *et al.*, 2013).

Afterwards, the different bands present in each membrane were quantified in reference to the parental line MDA-MB-231. Figure 4.1 shows that bands are less stained with mAb O-GlcNAC compared to the MDA-MB-231, establishing that there are less stained glycoproteins in these bands, except for band 2. Which is 1,921 and 1,131 times higher in MDA-MB-231/400nM and MDA-MB-231/1000nm, respectively. In HNK-1-stained membrane (Figure 4.2), we have obtained a different result, bands in both resistant cell lines exhibit an increased profile. These contain more glycoproteins than the bands obtained in the parental line. The Le[x]-stained membrane (Figure 4.3) displays loss and increase in the first and second band, respectively, in resistant cell lines. On the other hand, sLe[a]-stained membrane (Figure 4.4) does not demonstrate a different glycosylation pattern between sensitive and resistant cell lines. Ultimately, the membrane presented in Figure 4.5 manifests a decreasing motif in sLe[x]-stained glycoproteins.

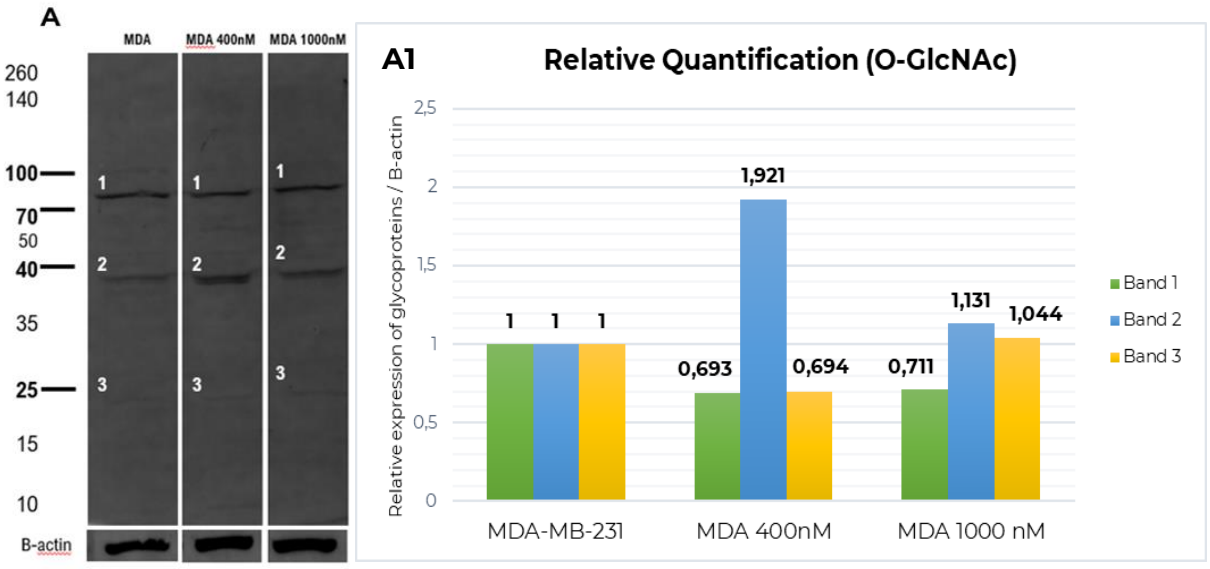


**Figure 4.1 - Western blot analysis of isolated membrane proteins from MDA-MB-231 cells, PAX-sensitive and PAX-resistant (400nM and 1000nM) stained with anti-O-GlcNAc and relative quantification of the western blot membrane stained with the same antibody. (A)** MDA: MDA-MB-231 PAX-sensitive cells; MDA 400nM: MDA-MB-231/400nM PAX-resistant cells; MDA 1000nM: MDA-MB-231/1000nM PAX-resistant cells; Molecular marker used Spectra Multicolour Broad Range Protein Ladder; β-actin protein expression level was analysed as loading control. The wells were loaded with 20ug of protein. Proteins were stained with mouse monoclonal antibodies. **(A1)** MDA-MB-231 PAX-sensitive cells are the reference bands; MDA 400nM: MDA-MB-231/400nM PAX-resistant cells; MDA 1000nM: MDA-MB-231/1000nM PAX-resistant cells. Result from 1 independent experiment.

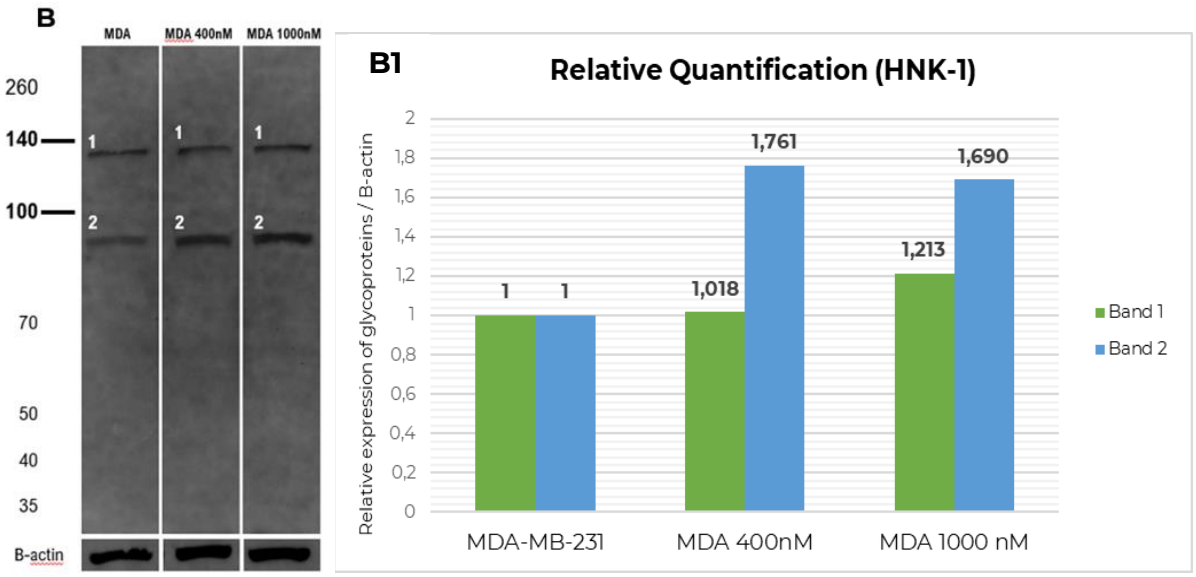


**Figure 4.2 - Western blot analysis of isolated membrane proteins from MDA-MB-231 cells, PAX-sensitive and PAX-resistant (400nM and 1000nM) stained with anti-O-HNK-1 and relative quantification of the western blot membrane stained with the same antibody. (B)** MDA: MDA-MB-231 PAX-sensitive cells; MDA 400nM: MDA-MB-231/400nM PAX-resistant cells; MDA 1000nM: MDA-MB-231/1000nM PAX-resistant cells; Molecular marker used Spectra Multicolour Broad Range Protein Ladder; β-actin protein expression level was analysed as loading control. The wells were loaded with 20ug of protein. Proteins were stained with mouse monoclonal antibodies. **(B1)** MDA-MB-231 PAX-sensitive cells are the reference bands; MDA 400nM: MDA-MB-231/400nM PAX-resistant cells; MDA 1000nM: MDA-MB-231/1000nM PAX-resistant cells. Result from 1 independent experiment.

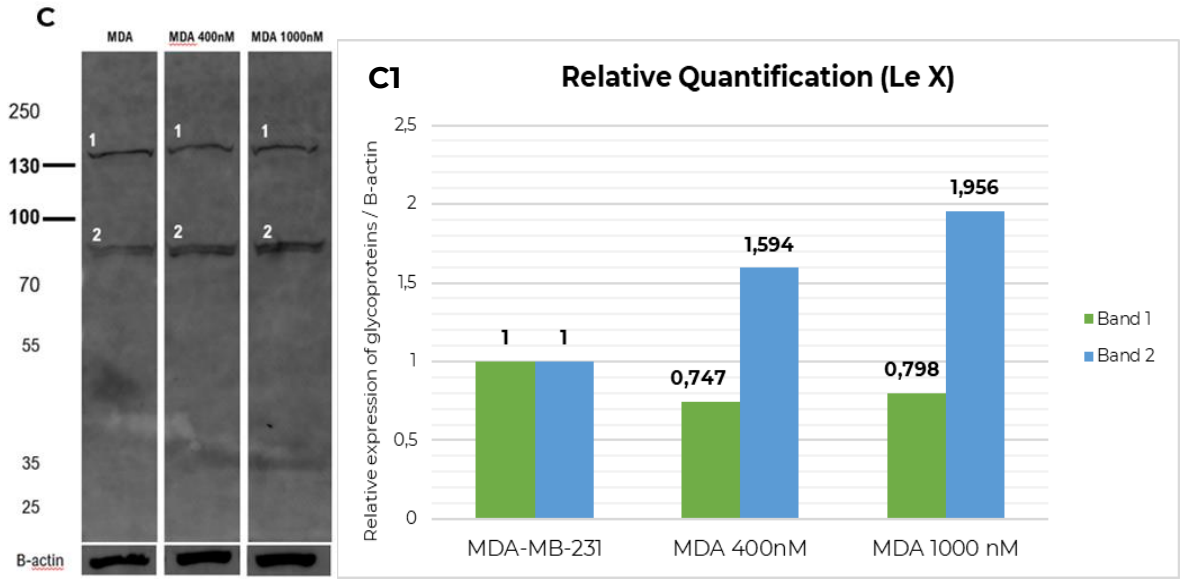


**Figure 4.3 - Western blot analysis of isolated membrane proteins from MDA-MB-231 cells, PAX-sensitive and PAX-resistant (400nM and 1000nM) stained with anti-Le X and relative quantification of the western blot membrane stained with the same antibody. (C)** MDA: MDA-MB-231 PAX-sensitive cells; MDA 400nM: MDA-MB-231/400nM PAX-resistant cells; MDA 1000nM: MDA-MB-231/1000nM PAX-resistant cells; Molecular marker used Page Ruler Plus Prestained Protein Ladder; β-actin protein expression level was analysed as loading control. The wells were loaded with 20ug of protein. Proteins were stained with mouse monoclonal antibodies. **(C1)** MDA-MB-231 PAX-sensitive cells are the reference bands; MDA 400nM: MDA-MB-231/400nM PAX-resistant cells; MDA 1000nM: MDA-MB-231/1000nM PAX-resistant cells. Result from 1 independent experiment.

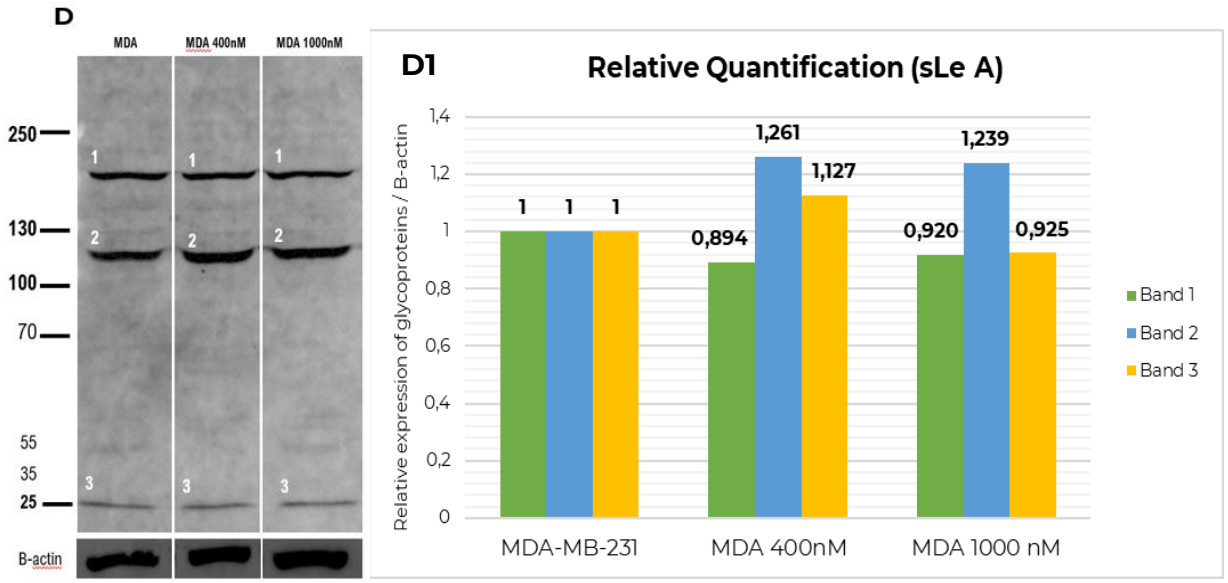


**Figure 4.4 - Western blot analysis of isolated membrane proteins from MDA-MB-231 cells, PAX-sensitive and PAX-resistant (400nM and 1000nM) stained with anti-sLe A and relative quantification of the western blot membrane stained with the same antibody. (D)** MDA: MDA-MB-231 PAX-sensitive cells; MDA 400nM: MDA-MB-231/400nM PAX-resistant cells; MDA 1000nM: MDA-MB-231/1000nM PAX-resistant cells; Molecular marker used Page Ruler Plus Prestained Protein Ladder; β-actin protein expression level was analysed as loading control. The wells were loaded with 20ug of protein. Proteins were stained with mouse monoclonal antibodies. **(D1)** MDA-MB-231 PAX-sensitive cells are the reference bands; MDA 400nM: MDA-MB-231/400nM PAX-resistant cells; MDA 1000nM: MDA-MB-231/1000nM PAX-resistant cells. Result from 1 independent experiment.

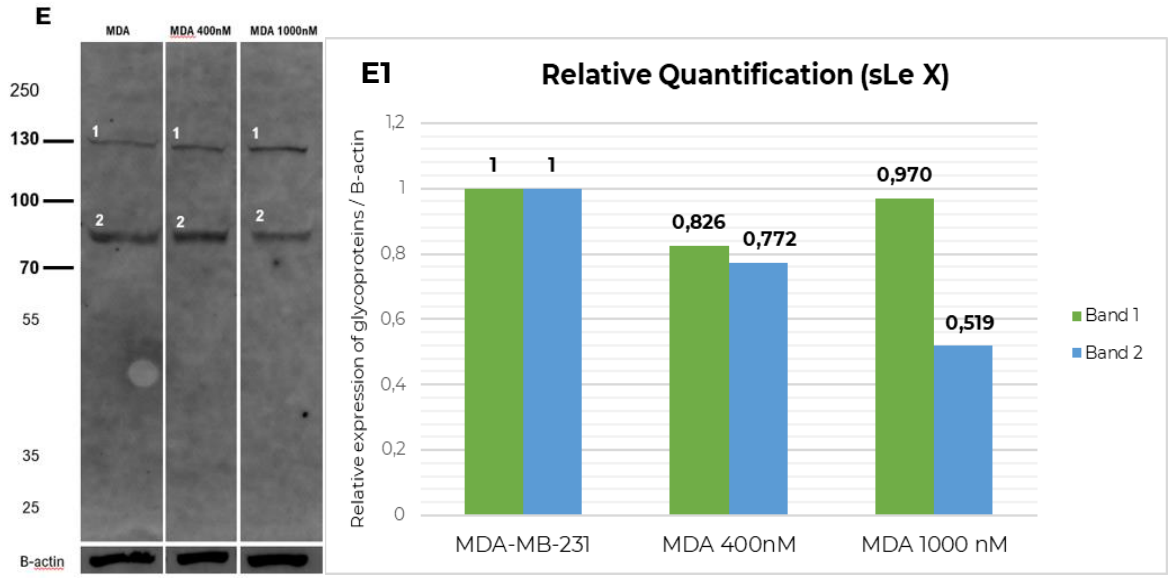


**Figure 4.5 - Western blot analysis of isolated membrane proteins from MDA-MB-231 cells, PAX-sensitive and PAX-resistant (400nM and 1000nM) stained with anti-sLe X and relative quantification of the western blot membrane stained with the same antibody. (E)** MDA: MDA-MB-231 PAX-sensitive cells; MDA 400nM: MDA-MB-231/400nM PAX-resistant cells; MDA 1000nM: MDA-MB-231/1000nM PAX-resistant cells; Molecular marker used Page Ruler Plus Prestained Protein Ladder; β-actin protein expression level was analysed as loading control. The wells were loaded with 20ug of protein. Proteins were stained with mouse monoclonal antibodies. **(E1)** MDA-MB-231 PAX-sensitive cells are the reference bands; MDA 400nM: MDA-MB-231/400nM PAX-resistant cells; MDA 1000nM: MDA-MB-231/1000nM PAX-resistant cells. Result from 1 independent experiment.

## 4.2 ASSESSMENT OF GENE EXPRESSION CHANGES IN PAX-RESISTANT BC CELL LINE

In the interest of evaluating changes in gene expression of proteins involved in human glycosylation in PAX resistant cells, specifically enzymes that affect glycosylation, 84 targeted genes were analysed via RT-PCR assays in both sensitive and resistant cell lines, MDA-MB-231 and MDA-MB-231/1000nM. Relative expression was determined using the $2^{-\Delta\Delta Ct}$ method (list of genes, respective Ct and Fold Change values showed in Annex 3 and Annex 4).

Between the two cell lines MDA-MB-231 and MDA-MB-231/1000nM, *A4GNT* (α-1,4-N-Acetylglucosaminyltransferase), *GALNT8* (ppN-Acetylgalactosaminyltransferase 8), *GALNT9* (ppN-Acetylgalactosaminyltransferase 8), *GALNTL5 (*ppN-Acetylgalactosaminyltransferase Like 5*), GALNTL6* (ppN-Acetylgalactosaminyltransferase Like 5), *NEU2* (Neuraminidase 2), *ST6GALNAC1* (ST6 N-Acetylgalactosaminide α-2,6-Sialyltransferase 1), *ST8SIA2* (ST8 α-N-Acetyl-Neuraminide α-2,8-Sialyltransferase 2) *and ST8SIA3* (ST8 α-N-Acetyl-Neuraminide α-2,8-Sialyltransferase 3) did not present amplification or showed low expression in both cell lines (see Table 7.4 and Table 7.5 in Annex 3 and Annex 4, respectively).

The only two genes found to be differently expressed in sensitive and resistant cells were *GALNT14* (ppN-Acetylgalactosaminyltransferase 14) and *MGAT3* (β-1,4-Mannosyl-Glycoprotein 4-β-N-Acetylglucosaminyltransferase). *GALNT14* is significantly downregulated while *MGAT3* had the opposite result, is significantly upregulated in MDA-MB-231/1000nM, Figure 4.6.

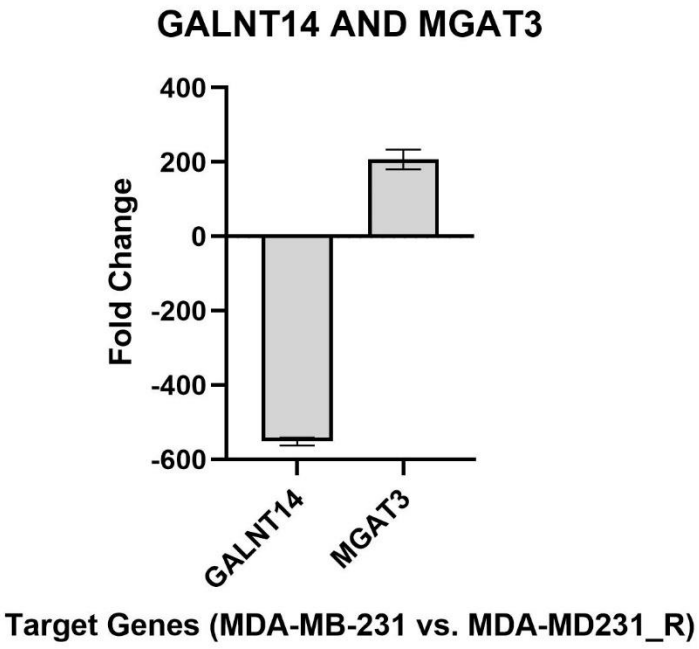


**Figure 4.6 - Genes differentially expressed in MDA-MB-231/1000nM resistant cell line in comparison to sensitive MDA-MD-231 parental line.** MDA-MB-231: sensitive parental line; MDA-MB-231_R: resistant MDA-MB-231/1000nM. Results are reported as Fold Change, which was obtained through calculating $2^{-\Delta\Delta Ct}$ values of the targeted genes from the RT-PCR assays. The graph was obtained using GraphPad Prism 9 software. Mean values ± standard error of the mean (SEM) are presented by error bars; a p-value<0.005 was considered statistically significant. GALNT14: ppN-Acetylgalactosaminyltransferase 14; MGAT3: β-1,4-Mannosyl-Glycoprotein 4-β-N-Acetylglucosaminyltransferase. Result from 3 independent experiments.

# 5. DISCUSSION AND CONCLUSIONS

CDR is a hindrance to long-term patient survival where cancer cells adopt distinct and diverse pathways to elude therapy-induced cell death and therefore acquire drug resistance. Cancer evolution and tumour heterogeneity determine this resistance development and, eventually, disease relapse, which has become a major problem in oncology. Drug resistance is defined as the inherited ability of cells to survive clinically relevant drug concentrations. There are several mechanisms underlying CDR, such as, drug efflux and inactivation, changes in drug metabolism, cell death inhibition, enhancement in DNA repair capacity, tumour heterogeneity (intra and inter-tumour heterogeneity), tumour microenvironment, EMT and epigenetic changes. Hence, tumour cells are recognized as drug-sensitive or drug-resistant (Chatterjee e Bivona, 2019; Haider *et al.*, 2020).

Glycosylation emerged as a further hallmark of neoplastic cells. Protein glycosylation is the most abundant PTM found on the majority of all secreted and cellular proteins, an enzymatic process that produces glycosidic bonds between monosaccharide moieties and proteins, or lipids, which has a role in every vital cellular process. Proteins pass through the ER/Golgi apparatus pathway and are catalysed by sequential coordinated glycosyltransferase and glycosidases to form the structures of the final glycosylated product. This process has long been associated with the development and progression of cancers. In tumour cells this enzymatic process is modified due to modifications in its glycome which results in an altered glycosylation pattern. Additionally, glycan biosynthesis depends upon bioavailability and abundance of glycosylation enzymes, substrates, and sugar donors. The obtained glycoproteins are involved in a wide number of molecular processes such as (1) cell recognition, (2) cell signalling, (3) cell-cell interaction, (4) cell-ECM and cell-cell adhesion, (5) protein folding, (6) protection against proteases and immune recognition, (7) membrane organization, among many other features. (Costa *et al.*, 2020; Thomas, Rathinavel e Radhakrishnan, 2021).

Cancer-associated differential glycosylation has been established and this dysregulation in the glycan biosynthetic pathway leads to aberrant glycosylation in tumour cells. The altered and atypical glycosylation pattern is due to aberrant expression and mislocalization of the responsible enzymes, as imbalances that affect the availability and abundance of sugar donors. The most prominently highlighted structural tumour-associated modifications in the literature are increase glycan branching, sialylation, and fucosylation, along with novel or truncated glycan structures. Which is interconnected

with cell's glycome under or overexpression. These modifications can end up favouring pathogenic tumour development, progression and metastasis, and also inherent cell-cell and cell-ECM interactions (Thomas, Rathinavel e Radhakrishnan, 2021).

PAX is a taxane widely used in the treatment of several solid tumours, such as BC, however, its employment during therapy may lead to CDR, and in consequence, tumour progression. Various mechanisms have been associated with PAX-resistance, however there is little consensus about the molecular mechanisms underlying this type of resistance (Esparza-Lopez *et al.*, 2022).

Previous studies demonstrate that there is a link between CDR mechanisms and chemoresistance, aberrant glycosylation and CDR, thus aberrant glycosylation is implicated in cancer chemoresistance. However, there is no mention concerning glycosylation in PAX-resistant tumour cells. Therefore, it is crucial to know the cause and underlying mechanisms of drug resistance, in order to develop CDR biomarkers.

To elucidate the mechanisms involved in aberrant glycosylation present in PAX-resistant cells, we analysed altered glycosylation patterns in BC cells. A PAX-resistant BC cell line was previously established by our group (Duarte, C., 2022) at three different concentrations, MDA-MB-231/400nM, MDA-MB-231/800nM and MDA-MB-231/1000nM. Resistance to PAX was developed by stepwise adaptation to increasing drug concentrations. During cell culture, MDA-MB-231/800nM cells started slowing down their growth rate and their morphology was considerably altered and, eventually, their survival in culture was no longer possible. Thus, we considered that resistance was not truly established or that while stored at -150°C cells lost resistance. Analysis proceeded with MDA-MB-231 parental cell line (PAX-sensitive), MDA-MB-231/400nM and MDA-MB-231/1000nM.

Studies show that several O-GlcNAc PTMs occur in proteins involved in various cellular functions, such as cell metabolism, signal transduction, transcriptional regulation, cell cycle control, protein trafficking and cell structure regulation (Lu *et al.*, 2022). Another important aspect is that this is a highly dynamic and reversible process. O-GlcNAc transferase (OGT) is responsible for attaching β-N-GlcNAc and β-Nacetylglucosaminidase (OGA) removes it (Lu *et al.*, 2022). An increase in O-GlcNAcylation is visualized in the second band (around 40 kDa) between MDA-MB-231 cells and MDA-MB-231/PAX, this correlates with the later statement. MDA-MB-231/400nM are glycosylated 1,921 times higher and MDA-MB-231/1000nM are 1,131 times, with reference to PAX-sensitive cells. This notorious increase harmonizes with the aberrant glycosylation pattern assumption in

CDR, promoting invasion and metastasis in BC. Ferrer et al. revealed that elevated O-GlcNAcylation promoted the invasion and metastasis of BC cells by regulating the sirtuin 1 (SIRT1)/extracellular regulated kinase (ERK)/ FOXM1 axis (Ferrer *et al.*, 2017). However, the bands obtained at higher (~80 kDa) and lower (~24 kDa) molecular weight, first and third band, respectively, exhibit a diminished number of glycoproteins O-GlcNAcylated. O-GlcNAcylation has not been related with resistance to PAX in BC cells, however our results suggest this particular PTM can be involved in PAX resistance.

Regarding the HNK-1 N-glycan, very few associations have been reported for BC and several questions remain unanswered. According to the literature, HNK-1 is one of the most characteristic glycoepitopes in the nervous system however, despite the highly neural specific expression, it is also expressed in extracellular adhesion molecules. This suggests that its function varies depending on the type of cancer (Morita *et al.*, 2008; Nakagawa *et al.*, 2012). Our results indicate an increase in band 2, in between 90 and 100 kDa, in both PAX resistant cell lines which may favour malignant tumour progression and invasion and, consequently, be linked to chemoresistance to PAX.

On the other hand, $Le^x$ staining reveals a consistent increase in band 2 with resistance, near 90 kDa. Results show that MDA-MB-231/400nM glycoproteins are glycosylated 1,594-fold higher and MDA-MB-231/1000nM are 1,956-fold higher, with reference to PAX-sensitive cells. The expression of $Le^x$ in certain BC cell lines is upregulated in tumour tissues and has been associated with poor prognosis (Koh *et al.*, 2013). This glycan epitopes present the three monosaccharides displayed in Lewis antigens, specifically, GlcNAc, Gal and Fuc, however, they are distinguished by carrying α1-3 Fuc residues, associated with the acquisition of increased fucosylation which is characteristic of tumour cells (Blanas *et al.*, 2018). The results suggest that glycoproteins in MDA-MB-231 resistant cell's glycocalyx are further terminal α1-3 fucosylated than MDA-MB-231 PAX-sensitive cells. This is in agreement with reports that associate $Le^X$ expression and BC metastasis, recognizing this antigen as a prominent biomarker in invading tumour tissues (Blanas *et al.*, 2018). This is also a good indicator that aberrant glycosylation is associated with BC acquired resistance, suggesting that $Le^x$ overexpression is involved in PAX-resistance mechanisms.

Concerning the two sialylated antigens, $sLe^a$ and $sLe^x$, the results obtained are not in agreement with literature reports regarding the type II and type I (α1-4 and α1-3 fucosylation) sialylated Lewis antigens, respectively. Since $sLe^a$ and $sLe^x$ are established cancer biomarkers, their expression levels tend to increase with advanced BC stage and

are involved in various inter and intracellular biological process, such as cell adhesion and intercommunication. Cazet et al., mention that downregulation of a sialyltransferase involved in $sLe^x$ assembly significantly decreases MDA-MB-231 cell migration (Cazet *et al.*, 2010). Thus, these glycan biomarkers participate in metastasis, as they allow the interaction between tumour cells with selectins expressed in non-diseased endothelial cells (Blanas *et al.*, 2018). Our results demonstrate that $sLe^a$ expression was not differentiated in MDA-MB-231/400nM and MDA-MB-231/1000nM cells and $sLe^x$ had the opposite result, seeing that the number of glycosylated proteins diminished with increasing PAX-resistant concentrations. Taking into account that the glycoproteins present in the obtained band are unknown we were not able to determine what influenced these contradictory results. In the future, it is important to identify the actual glycoproteins extracted from MDA-MB-231 cells since we can only propose that they are aberrantly glycosylated, which results in higher molecular weight bands (within 120 and 240 kDa in $sLe^a$ and within 80 and 130 kDa in $sLe^x$). Glycoproteins that could be considered are ABC transporters, such as ABCG2, this protein has a predicted molecular mass of 72 kDa and has three possible N-glycosylation sites in its extracellular loops (Diop e Hrycyna, 2005). Although, in chemoresistant cells this glycoprotein can be further glycosylated and thus, have a superior molecular weight.

To our knowledge, no studies that associate protein glycosylation expression with resistance to PAX have been published, thus, it is not possible to compare our results with the literature.

Nevertheless, it is noticeable that glycocalyx glycosylation impacts BC cell's behaviour and modifications at this level affect the carbohydrates present in glycoproteins, expressing tumour-associated carbohydrate antigens (TACAs). Thus, malignant cells resort to different glycosylation mechanisms in order to become invasive, survive and progress to develop chemoresistance (Cazet *et al.*, 2010).

New approaches have been explored to identify cancer biomarkers, especially in CDR. Glycoproteomic strategies are one of them since aberrant glycosylation is a hallmark of cancer and tumour glycome analysis could provide information about the involved enzymes in aberrant expression, such as glycosyltransferases and glycosidases. Potapenko et al., resorting to glycogene expression in BC, correlated 419 glycogenes with diagnosis, progression, and survival (Greville *et al.*, 2016). Therefore, the comparison of differential expression of these enzymes in BC cells and in BC-resistant cells may help us

identify specific resistance-associated aberrations in glycan structures and favour new biomarker candidates.

In order to evaluate if there are changes in enzyme gene expression involved in human glycosylation in PAX-resistant cells, we analysed the glycome of MDA-MB-231 cells, as the PAX-sensitive cell line, and of MDA-MB-231/1000nM, the previously established PAX-resistant cell line. The comparison between these two cell lines displays the changes in glycoprotein expression caused by resistance to PAX.

Only two genes were differentially expressed in these two BC cell lines, *GALNT14* was downregulated while *MGAT3* was upregulated in MDA-MB-231/1000nM cells.

As mentioned before, O-glycosylation is one of the major types of glycosylation widely found in proteins in the secretory pathway and N-acetylgalactosaminyltransferase (GALNT) is the glycosyltransferase family that initiates this PTM in the Golgi apparatus, adding a N-acetylgalactosamine (GalNAc) to the Ser or Thr residue in proteins (Lin e Yeh, 2020). This extensive family consists of at least 20 enzymes, namely, GALNT1 to 14 and from GANLTL1 to L6, all these have different substrates and expression patterns having diverse roles in carcinogenesis and tumour metastasis (Lin e Yeh, 2020). There are not many studies regarding the role of GALNTs in CDR, however, modifications in the O-glycosylation pattern are associated with a variety of developments in epithelial defects and neoplasms. GALNTs influence a wide spectrum of biological functions, such as cell-ECM interactions, altered receptors communication (resistance to apoptosis-inducing ligands during oncogenesis), alteration of vesicle trafficking genes and O-glycosylation (COPI-based translocation of GalNAcTs to the ER) (Ramzan *et al.*, 2016). GALNT14 has been reported in BC, specifically, to be over-expressed in 83,9% of BC tissues, and its expression regulates MDR in BC cells (Lin e Yeh, 2020). Nevertheless, a higher histological grade of invasive ductal carcinoma is linked to a lower expression level of GALNT14, high-grade cancer cells are more prone to invasiveness and metastasis. A putative pro-tumorigenesis mechanism shows that decreased GALNT14 O-glycosylation of proapoptotic death receptors suppresses the clustering of TRAIL (tumour necrosis factor-related apoptosis-inducing ligand), disturbing apoptosis induction (Ramzan *et al.*, 2016). Studies show that this glycosyltransferase promotes BC metastasis to the lungs and regulates the stability of ABCB1 (Lin e Yeh, 2020). On the other hand, Wu et al., demonstrated that Osterix decreased the BC cells' chemosensitivity by upregulating the expression of GALNT14, which eventually suppressed their apoptosis (Wu *et al.*, 2017). Considering all these findings and our analysed results, GALNT14 downregulation may be implicated in PAX

chemoresistance, furthermore it retains a significant role in CDR mechanisms interrelated with PAX-resistance MDA-MB-231 cells. Suggesting again that aberrant glycosylation is implicated in cancer chemoresistance.

On another note, we have differential expression in a glycosyltransferase family, N-acetylglucosaminyltransferases (GlcNAcT), precisely, N-acetylglucosaminyltransferase III (MGAT3). This enzyme is highly involved in N-glycosylation, it transfers a GlcNAc monosaccharide in a β4-linkage to the mannose core of complex or hybrid N-glycans, which generates a bisecting GlcNAc structure, altering the glycan conformation and therefore recognition (Kohler *et al.*, 2016). Studies show that bisecting GlcNAc inhibits the action of α-mannosidase II trimming and GlcNacT-II, GlcNacT-IV and GlcNacT-V, developing hybrid structures and elongated/branched N-glycans, respectively. However, the role of MGAT3/bisecting GlcNAc in cancer is dysregulated and probably differs taking into account distinct cancers since it may function as a promoter or suppressor of cell migration and cell adhesion (Cheng *et al.*, 2020).

Altogether, our data suggest that altered glycosylation occurs during the development of resistance to PAX in BC. Our data identify two genes as possible biomarkers of PAX resistance, *GALNT14* and *MGAT3*. Further studies are required to confirm their importance in PAX resistance, namely by immunohistochemical analysis, a technique that allows us to relate expression of specific glycan structures and potentially identify biomarkers with clinical cancer features and other glycoengineering methods, such as flow cytometry combined with glycan-based inhibitors which enables an impairment on tumour cells' glycome and its capacity to grow and metastasize, further confirming the importance of these genes in PAX-resistant BC cells. In the future, we would like to compare the variations in glycosylation patterns in both membrane and cytosolic proteins, in other BC subtypes and in a non-tumorigenic epithelial cell line, using the previous mentioned glycoengineering method. Nonetheless, it is important to consider the complexity of glycan biosynthesis and the fact that it is a non-template process hence the impairment in further progress. On a more positive note, understanding the inherent mechanisms that impact both glycosylation and CDR in tumorigenesis may reveal promising new targets and biomarkers of CDR.

# 6. BIBLIOGRAPHY

ALQAHTANI, Fulwah Yahya *et al.* - Paclitaxel. **Profiles of Drug Substances, Excipients and Related Methodology**. . ISSN 18715125. 44:2019) 205–238. doi: 10.1016/bs.podrm.2018.11.001.

ANDERGASSEN, Ulrich *et al.* - Glycosyltransferases as Markers for Early Tumorigenesis. **BioMed Research International**. . ISSN 23146141. 2015:2015). doi: 10.1155/2015/792672.

Bellis SL, Reis CA, Varki A, et al. **Glycosylation Changes in Cancer**. In: Varki A, Cummings RD, Esko JD, et al., editors. **Essentials of Glycobiology** [Internet]. 4th edition. Cold Spring Harbor (NY): Cold Spring Harbor Laboratory Press; 2022. Chapter 47.

BLANAS, Athanasios *et al.* - Fucosylated antigens in cancer: An alliance toward tumor progression, metastasis, and resistance to chemotherapy. **Frontiers in Oncology**. . ISSN 2234943X. 8:FEB (2018) 1–14. doi: 10.3389/fonc.2018.00039.

Brockhausen I, Wandall HH, Hagen KGT, et al. **O-GalNAc Glycans**. In: Varki A, Cummings RD, Esko JD, et al., editors. **Essentials of Glycobiology** [Internet]. 4th edition. Cold Spring Harbor (NY): Cold Spring Harbor Laboratory Press; 2022. Chapter 10.

BUKOWSKI, Karol; KCIUK, Mateusz; KONTEK, Renata - Mechanisms of multidrug resistance in cancer chemotherapy. **International Journal of Molecular Sciences**. . ISSN 14220067. 21:9 (2020). doi: 10.3390/ijms21093233.

CAZET, Aurélie *et al.* - Consequences of the expression of sialylated antigens in breast cancer. **Carbohydrate Research**. . ISSN 00086215. 345:10 (2010) 1377–1383. doi: 10.1016/j.carres.2010.01.024.

CHATTERJEE, Nilanjana; BIVONA, Trever G. - Polytherapy and Targeted Cancer Drug Resistance. **Trends in Cancer**. . ISSN 24058033. 5:3 (2019) 170–182. doi: 10.1016/j.trecan.2019.02.003.

CHENG, Lanming *et al.* - Bisecting N-Acetylglucosamine on EGFR Inhibits Malignant Phenotype of Breast Cancer via Down-Regulation of EGFR/Erk Signaling. **Frontiers in Oncology**. . ISSN 2234943X. 10:June (2020) 1–14. doi: 10.3389/fonc.2020.00929.

CHEUNG, Kwok-Leung - Treatment Strategies and Survival Outcomes in Breast Cancer. 2020) 12–15. doi: 10.3390/cancers12030735.

COSTA, Ana Filipa *et al.* - Targeting Glycosylation: A New Road for Cancer Drug Discovery. **Trends in Cancer**. . ISSN 24058033. 6:9 (2020) 757–766. doi: 10.1016/j.trecan.2020.04.002.

DINIZ, Francisca *et al.* - Glycans as Targets for Drug Delivery in Cancer. **Cancers**. . ISSN 20726694. 14:4 (2022) 1–19. doi: 10.3390/cancers14040911.

DIOP, Ndeye K.; HRYCYNA, Christine A. - N-linked glycosylation of the human ABC transporter ABCG2 on asparagine 596 is not essential for expression, transport activity, or trafficking to the plasma membrane. **Biochemistry**. . ISSN 00062960. 44:14 (2005) 5420–5429. doi: 10.1021/bi0479858.

EAVARONE, David A. *et al.* - Humanized anti-Sialyl-Tn antibodies for the treatment of ovarian carcinoma. **PLoS ONE**. . ISSN 19326203. 13:7 (2018) 1–18. doi:

10.1371/journal.pone.0201314.

ESPARZA-LOPEZ, José *et al.* - Paclitaxel resistance is mediated by NF-κB on mesenchymal primary breast cancer cells. **Oncology Letters**. . ISSN 17921082. 23:2 (2022) 1–10. doi: 10.3892/ol.2021.13168.

FERLAY, Jacques *et al.* - Cancer statistics for the year 2020: An overview. **International Journal of Cancer**. . ISSN 10970215. 149:4 (2021) 778–789. doi: 10.1002/ijc.33588.

FERRER, C. M. *et al.* - O-GlcNAcylation regulates breast cancer metastasis via SIRT1 modulation of FOXM1 pathway. **Oncogene**. . ISSN 14765594. 36:4 (2017) 559–569. doi: 10.1038/onc.2016.228.

FONSECA, Leonardo Marques DA *et al.* - Glycosylation in cancer: Interplay between multidrug resistance and epithelial-to-mesenchymal transition? **Frontiers in Oncology**. . ISSN 2234943X. 6:JUN (2016) 1–10. doi: 10.3389/fonc.2016.00158.

Gagneux P, Hennet T, Varki A. **Biological Functions of Glycans**. In: Varki A, Cummings RD, Esko JD, et al., editors. **Essentials of Glycobiology** [Internet]. 4th edition. Cold Spring Harbor (NY): Cold Spring Harbor Laboratory Press; 2022. Chapter 7.

GREVILLE, Gordon *et al.* - Epigenetic regulation of glycosylation and the impact on chemo-resistance in breast and ovarian cancer. **Epigenetics**. . ISSN 15592308. 11:12 (2016) 845–857. doi: 10.1080/15592294.2016.1241932.

HAIDER, Tanweer *et al.* - Drug resistance in cancer: mechanisms and tackling strategies. **Pharmacological Reports**. . ISSN 17341140. 72:5 (2020) 1125–1151. doi: 10.1007/s43440-020-00138-7.

HARBECK, Nadia *et al.* - **Breast cancer**. ISBN 0123456789.

International Agency for Research on Cancer. Global Cancer Observatory. Cancer Today [Internet]. 2020 [cited Novembre 14, 2022]. https://gco.iarc.fr/today/home

KAMPAN, Nirmala Chandralega *et al.* - Paclitaxel and its evolving role in the management of ovarian cancer. **BioMed Research International**. . ISSN 23146141. 2015:2015). doi: 10.1155/2015/413076.

KHOSROWABADI, Elham *et al.* - Altered glycosylation of several metastasis-associated glycoproteins with terminal GalNAc defines the highly invasive cancer cell phenotype. **Oncotarget**. . ISSN 19492553. 13:2022) 73–89. doi: 10.18632/ONCOTARGET.28167.

KOH, Young Wha *et al.* - Expression of Lewis X is associated with poor prognosis in triple-negative breast cancer. **American Journal of Clinical Pathology**. . ISSN 00029173. 139:6 (2013) 746–753. doi: 10.1309/AJCP2E6QNDIDPTTC.

KOHLER, Reto S. *et al.* - Epigenetic activation of MGAT3 and corresponding bisecting GlcNAc shortens the survival of cancer patients. **Oncotarget**. . ISSN 19492553. 7:32 (2016) 51674–51686. doi: 10.18632/oncotarget.10543.

Lebrilla CB, Liu J, Widmalm G, et al. **Oligosaccharides and Polysaccharides.** In: Varki A, Cummings RD, Esko JD, et al., editors. **Essentials of Glycobiology** [Internet]. 4th edition. Cold Spring Harbor (NY): Cold Spring Harbor Laboratory Press; 2022. Chapter 3.

LI, Ying Jie *et al.* - Autophagy and multidrug resistance in cancer. **Chinese journal of cancer**. . ISSN 1944446X. 36:1 (2017) 52. doi: 10.1186/s40880-017-0219-2.

LIN, Wey Ran; YEH, Chau Ting - GALNT14: An emerging marker capable of predicting therapeutic outcomes in multiple cancers. **International Journal of Molecular Sciences**. . ISSN 14220067. 21:4 (2020) 1–12. doi: 10.3390/ijms21041491.

LIU, Huimin *et al.* - Advances in molecular mechanisms of drugs affecting abnormal glycosylation and metastasis of breast cancer. **Pharmacological Research**. . ISSN 10961186. 155:1066 (2020). doi: 10.1016/j.phrs.2020.104738.

LOIBL, Sibylle *et al.* - Breast cancer. **The Lancet**. . ISSN 1474547X. 397:10286 (2021) 1750–1769. doi: 10.1016/S0140-6736(20)32381-3.

LONGACRE, Mckenna; SNYDER, Nicole; SARKAR, Sibaji - Drug Resistance in Cancer : An Overview. 2014) 1769–1792. doi: 10.3390/cancers6031769.

LU, Qingsong *et al.* - O-GlcNAcylation: an important post-translational modification and a potential therapeutic target for cancer therapy. **Molecular Medicine**. . ISSN 15283658. 28:1 (2022). doi: 10.1186/s10020-022-00544-y.

MA, Zhi *et al.* - Expression of the Carbohydrate Lewis Antigen, Sialyl Lewis A, Sialyl Lewis X, Lewis X, and Lewis Y in the Placental Villi of Patients With Unexplained Miscarriages. **Frontiers in Immunology**. . ISSN 16643224. 12:May (2021) 1–12. doi: 10.3389/fimmu.2021.679424.

MALONEY, Sara M. *et al.* - Mechanisms of taxane resistance. **Cancers**. . ISSN 20726694. 12:11 (2020) 1–57. doi: 10.3390/cancers12113323.

MANSOORI, Behzad *et al.* - The different mechanisms of cancer drug resistance: A brief review. **Advanced Pharmaceutical Bulletin**. . ISSN 22517308. 7:3 (2017) 339–348. doi: 10.15171/apb.2017.041.

MEANY, Danni L.; CHAN, Daniel W. - Aberrant glycosylation associated with enzymes as cancer biomarkers. **Clinical Proteomics**. . ISSN 15426416. 8:1 (2011) 1–14. doi: 10.1186/1559-0275-8-7.

MEHRGOU, Amir; AKOUCHEKIAN, Mansoureh - The importance of BRCA1 and BRCA2 genes mutations in breast cancer development. **Medical Journal of the Islamic Republic of Iran (MJIRI) Iran University of Medical Sciences**. 30:369:2016).

MORITA, Ippei *et al.* - Expression and function of the HNK-1 carbohydrate. **Journal of Biochemistry**. . ISSN 0021924X. 143:6 (2008) 719–724. doi: 10.1093/jb/mvm221.

MUNKLEY, Jennifer; ELLIOTT, David J. - Hallmarks of glycosylation in cancer. **Oncotarget**. . ISSN 19492553. 7:23 (2016) 35478–35489. doi: 10.18632/oncotarget.8155.

NAKAGAWA, Naoki *et al.* - Human natural killer-1 sulfotransferase (HNK-1ST)-induced sulfate transfer regulates laminin-binding glycans on α-dystroglycan. **Journal of Biological Chemistry**. . ISSN 00219258. 287:36 (2012) 30823–30832. doi: 10.1074/jbc.M112.363036.

NĚMCOVÁ-FÜRSTOVÁ, Vlasta *et al.* - Characterization of acquired paclitaxel resistance of breast cancer cells and involvement of ABC transporters. **Toxicology and Applied Pharmacology**. . ISSN 10960333. 310:2016) 215–228. doi: 10.1016/j.taap.2016.09.020.

PINHO, Salomé S.; REIS, Celso A. - Glycosylation in cancer: Mechanisms and clinical implications. **Nature Reviews Cancer**. . ISSN 14741768. 15:9 (2015) 540–555. doi: 10.1038/nrc3982.

RAMZAN, Muhammad *et al.* - N -acetylgalactosaminyltransferases in cancer. 7:33 (2016).
REILY, Colin *et al.* - Glycosylation in health and disease. **Nature Reviews Nephrology**. . ISSN 1759507X. 15:6 (2019) 346–366. doi: 10.1038/s41581-019-0129-4.

Rini JM, Moremen KW, Davis BG, et al. **Glycosyltransferases and Glycan-Processing Enzymes.** In: Varki A, Cummings RD, Esko JD, et al., editors. **Essentials of Glycobiology** [Internet]. 4th edition. Cold Spring Harbor (NY): Cold Spring Harbor Laboratory Press; 2022. Chapter 6.

RITCHIE, Hannah; SPOONER, Fiona; ROSER, Max - **Causes of death** [Em linha], atual. 2018. Disponível em WWW:<URL:https://ourworldindata.org/causes-of-death>.

SAMAAN, Tala M. Abu *et al.* - Paclitaxel ' s Mechanistic and Clinical E ff ects on Breast Cancer. [s.d.]) 1–22.

SCHJOLDAGER, Katrine T. *et al.* - Global view of human protein glycosylation pathways and functions. **Nature Reviews Molecular Cell Biology**. . ISSN 14710080. 21:12 (2020) 729–749. doi: 10.1038/s41580-020-00294-x.

SCOTT, Danielle A.; DRAKE, Richard R. - Glycosylation and its implications in breast cancer. **Expert Review of Proteomics**. . ISSN 17448387. 16:8 (2019) 665–680. doi: 10.1080/14789450.2019.1645604.

Seeberger PH. **Monosaccharide Diversity.** In: Varki A, Cummings RD, Esko JD, et al., editors. **Essentials of Glycobiology** [Internet]. 4th edition. Cold Spring Harbor (NY): Cold Spring Harbor Laboratory Press; 2022. Chapter 2.

SILSIRIVANIT, Atit - Glycosylation markers in cancer. **Advances in Clinical Chemistry**. . ISSN 21629471. 89:2019) 189–213. doi: 10.1016/bs.acc.2018.12.005.

Stanley P, Moremen KW, Lewis NE, et al. **N-Glycans.** In: Varki A, Cummings RD, Esko JD, et al., editors. **Essentials of Glycobiology** [Internet]. 4th edition. Cold Spring Harbor (NY): Cold Spring Harbor Laboratory Press; 2022. Chapter 9.

THOMAS, Divya; RATHINAVEL, Ashok Kumar; RADHAKRISHNAN, Prakash - Altered glycosylation in cancer: A promising target for biomarkers and therapeutics. **Biochimica et Biophysica Acta - Reviews on Cancer**. . ISSN 18792561. 1875:1 (2021) 1–48. doi: 10.1016/j.bbcan.2020.188464.

Varki A, Cummings RD, Esko JD, et al., editors. **Essentials of Glycobiology** [Internet]. 4th edition. Cold Spring Harbor (NY): Cold Spring Harbor Laboratory Press; 2022.

WANG, Huabo *et al.* - HHS Public Protein glycosylation in cancer. **Annu Rev Pathol**. . ISSN 0036-8075. 2:2 (2015) 473–510. doi: 10.1146/annurev-pathol-012414-040438.Protein.

WANG, Xuan; ZHANG, Haiyun; CHEN, Xiaozhuo - Drug resistance and combating drug resistance in cancer. **Cancer Drug Resistance**. . ISSN 2578532X. 2:2 (2019) 141–160. doi: 10.20517/cdr.2019.10.

WU, Jiahui *et al.* - Osterix Decreases the Chemosensitivity of Breast Cancer Cells by Upregulating GALNT14. **Cellular Physiology and Biochemistry**. . ISSN 14219778. 44:3 (2017) 998–1010. doi: 10.1159/000485400.

## 7. ANNEXES

# ANNEX 1 – Materials related with Glycosylation Pattern analysis

**Table 7.1 – Recipe for the preparation of SDS-PAGE gel, both Resolving and Stacking gel.**

| Solution | Resolving 8% | | Stacking 4% | |
|---|---|---|---|---|
| | 1 Gel | 2 Gels | 1 Gel | 2 Gels |
| dH2O | 4,6 mL | 9,2 mL | 1,8 mL | 3,6 mL |
| 30% Acrylamide | 2,67 mL | 5,3 mL | 402 µL | 804 µL |
| 1,5M Tris pH 8,8 / 0,5M Tris pH 6,8 | 2,5 mL | 5 mL | 750 µL | 1,5 mL |
| 10% SDS | 100 µL | 200 µL | 30 µL | 60 µL |
| 10% APS (Amonium Persulfate) | 100 µL | 200 µL | 30 µL | 60 µL |
| TEMED | 10 µL | 20 µL | 3 µL | 6 µL |

**Table 7.2 – Staining Solutions for polyacrylamide gel staining**

| Reagent | Preparation |
|---|---|
| 3% Acetic Acid | Mix 30 mL of glacial acetic acid with 970 mL of ultrapure water |
| 50% Methanol | Mix 250 mL of methanol with 250 mL of ultrapure water |
| Oxidizing Solution | Add 250 mL of 3% acetic acid to the bottle labeled “Oxidizing Reagent”, then mix until material is completely dissolved |
| Reducing Solution | Add 250 mL of ultrapure water to the bottle labeled “Reducing Reagent”, then mix until material is completely dissolved |

# ANNEX 2

**Table 7.3 – Gene symbol layout for each target in TaqMan Array Human Glycosylation Plate.**

| | 1 | 2 | 3 | 4 | 5 | 6 | 7 | 8 | 9 | 10 | 11 | 12 |
|---|---|---|---|---|---|---|---|---|---|---|---|---|
| **A** | 18S | A4GNT | AGA | B3GLCT | B3GNT2 | B3GNT3 | B3GNT4 | B3GNT8 | B4GALT1 | B4GALT2 | B4GALT3 | B4GALT5 |
| **B** | C1GALT1 | C1GALT1C1 | EDEM1 | EDEM2 | EDEM3 | FUCA1 | FUCA2 | FUT11 | FUT8 | GALNT1 | GALNT10 | GALNT11 |
| **C** | GALNT12 | GALNT13 | GALNT14 | GALNT2 | GALNT3 | GALNT4 | GALNT6 | GALNT7 | GALNT8 | GALNT9 | GALNT16 | GALNTL5 |
| **D** | GALNTL6 | GANAB | GCNT1 | GCNT3 | GCNT4 | GLB1 | GNPTAB | GNPTG | HEXA | HEXB | MAN1A1 | MAN1A2 |
| **E** | MAN1B1 | MAN1C1 | MAN2A1 | MAN2A2 | MAN2B1 | MANBA | MGAT1 | MGAT2 | MGAT3 | MGAT4A | MGAT4B | MGAT4C |
| **F** | MGAT5 | MGAT5B | MOGS | NAGPA | NEU1 | NEU2 | NEU3 | NEU4 | OGT | POFUT1 | POFUT2 | POMGNT1 |
| **G** | POMT1 | POMT2 | PRKCSH | ST3GAL1 | ST3GAL2 | ST6GAL1 | ST6GALNAC1 | ST8SIA2 | ST8SIA3 | ST8SIA4 | ST8SIA6 | UGGT1 |
| **H** | UGGT2 | GAPDH | HPRT1 | GUSB | ACTB | B2M | HMBS | IPO8 | PGK1 | RPLP0 | TBP | TFRC |

## ANNEX 3

**Table 7.4 - Ct values obtained for each target in each array.** "Undetermined" states for the genes that were not amplificated; Statistical significance is presented with *.

| TARGET GENE | MDA-MB-231 (1) | MDA-MB-231 (2) | MDA-MB-231/1000NM (1) | MDA-MB-231/1000NM (2) |
|---|---|---|---|---|
| **18S** | 11,560108 | 9,684771 | 11,742515 | 12,417316 |
| **A4GNT** | Undetermined | Undetermined | Undetermined | 38 |
| **AGA** | 24,76786 | 24,929737 | 24,575089 | 24,384819 |
| **B3GLCT** | 25,484304 | 25,586538 | 25,163292 | 24,922827 |
| **B3GNT2** | 26,32872 | 26,30442 | 26,041605 | 25,796413 |
| **B3GNT3** | 30,149385 | 30,245941 | 29,406748 | 29,273003 |
| **B3GNT4** | 29,920374 | 29,897043 | 28,58123 | 28,44031 |
| **B3GNT8** | 29,584013 | 29,499046 | 29,771603 | 29,984486 |
| **B4GALT1** | 23,63638 | 23,89291 | 23,063805 | 23,07816 |
| **B4GALT2** | 25,462152 | 25,602005 | 25,201069 | 25,277416 |
| **B4GALT3** | 25,021074 | 25,29827 | 24,603994 | 24,603907 |
| **B4GALT5** | 24,240824 | 24,385202 | 24,111368 | 24,111599 |
| **CIGALT1** | 24,632034 | 24,382046 | 24,34922 | 24,151442 |
| **CIGALT1C1** | 33,51017 | 33,692997 | 33,072556 | 33,306526 |
| **EDEM1** | 23,036415 | 23,194681 | 23,56629 | 23,675653 |
| **EDEM2** | 25,602222 | 25,615599 | 25,28824 | 25,26509 |
| **EDEM3** | 25,229877 | 25,491007 | 25,696308 | 25,722782 |
| **FUCA1** | 24,546656 | 24,548426 | 24,56013 | 25,053185 |
| **FUCA2** | 22,73633 | 22,806602 | 22,817064 | 23,389467 |
| **FUT11** | 26,234144 | 26,321056 | 26,593636 | 26,779692 |
| **FUT8** | 24,02798 | 23,936974 | 24,210527 | 24,31929 |
| **GALNT1** | 24,133081 | 24,231936 | 23,135147 | 23,118357 |
| **GALNT10** | 25,693714 | 25,89236 | 25,90545 | 26,24284 |
| **GALNT11** | 26,000103 | 25,94375 | 25,977724 | 26,896223 |
| **GALNT12** | 28,975714 | 29,14211 | 28,147524 | 28,768307 |
| **GALNT13** | 27,960104 | 28,139484 | 27,853569 | 28,910007 |
| **GALNT14*** | 26,83342 | 27,586681 | 36,474022 | 36,435734 |
| **GALNT2** | 27,956514 | 28,061127 | 28,124187 | 29,35798 |
| **GALNT3** | 24,302076 | 24,56198 | 24,7565 | 25,403212 |
| **POC1B-GALNT4,GALNT4** | 26,452755 | 26,546429 | 26,360407 | 27,02459 |
| **GALNT6** | 24,831568 | 25,12463 | 24,811739 | 25,680716 |
| **GALNT7** | 25,635288 | 25,878325 | 25,392319 | 26,300812 |
| **GALNT8** | Undetermined | 37,052334 | 34,521637 | 35,18386 |
| **GALNT9** | Undetermined | Undetermined | Undetermined | 38 |
| **GALNT16** | 34,906208 | 35,21952 | 33,2116 | 34,94214 |
| **GALNTL5** | Undetermined | Undetermined | Undetermined | Undetermined |

| | | | | |
|---|---|---|---|---|
| **GALNTL6** | Undetermined | Undetermined | Undetermined | Undetermined |
| **GANAB** | 21,912745 | 21,975939 | 21,62621 | 22,323435 |
| **GCNT1** | 28,989265 | 28,961664 | 28,42667 | 28,91974 |
| **GCNT3** | 30,311298 | 30,163677 | 28,245335 | 28,728085 |
| **GCNT4** | 28,257486 | 28,46717 | 27,36299 | 27,79362 |
| **GLB1** | 23,727411 | 23,962425 | 23,742958 | 24,187782 |
| **GNPTAB** | 24,676807 | 24,683598 | 24,428947 | 24,988317 |
| **GNPTG** | 24,034046 | 24,23663 | 24,045322 | 24,55071 |
| **HEXA** | 23,371775 | 23,65322 | 22,961048 | 23,668686 |
| **HEXB** | 22,442787 | 22,335693 | 22,373125 | 22,703568 |
| **MAN1A1** | 26,008991 | 26,005163 | 25,909494 | 26,140497 |
| **MAN1A2** | 25,106169 | 25,301342 | 25,58049 | 26,101002 |
| **MAN1B1** | 24,497763 | 24,727907 | 24,052303 | 24,824356 |
| **MAN1C1** | 34,586964 | 35,27984 | 33,435303 | 34,000954 |
| **MAN2A1** | 23,97412 | 24,135073 | 23,548094 | 24,095472 |
| **MAN2A2** | 26,807121 | 26,963793 | 26,550713 | 27,256254 |
| **MAN2B1** | 25,249792 | 25,411047 | 25,096191 | 25,736246 |
| **MANBA** | 26,347832 | 26,642271 | 26,164457 | 26,656672 |
| **MGAT1** | 23,339977 | 23,240074 | 22,98826 | 23,452158 |
| **MGAT2** | 27,340431 | 27,98047 | 27,479311 | 28,980917 |
| **MGAT3*** | 37,70974 | 38 | 30,173817 | 30,437574 |
| **MGAT4A** | 29,964577 | 30,048006 | 28,527363 | 28,889948 |
| **MGAT4B** | 22,352701 | 22,328913 | 21,519396 | 22,247932 |
| **MGAT4C** | 36,64572 | 37,518555 | 38 | 37,61729 |
| **MGAT5** | 25,827787 | 26,252535 | 25,94769 | 26,30129 |
| **MGAT5B** | 29,633963 | 29,882122 | 29,331398 | 29,92395 |
| **MOGS** | 26,601278 | 26,796417 | 27,12639 | 27,837103 |
| **NAGPA** | 25,759356 | 26,040747 | 25,034378 | 25,666878 |
| **NEU1** | 26,13138 | 26,336716 | 25,556328 | 26,190683 |
| **NEU2** | 37,30623 | Undetermined | Undetermined | Undetermined |
| **NEU3** | 30,503386 | 30,84071 | 29,716814 | 30,253147 |
| **NEU4** | 32,41051 | 32,80018 | 32,761333 | 33,054707 |
| **OGT** | 22,244772 | 22,479023 | 21,394026 | 21,814577 |
| **POFUT1** | 24,272743 | 24,667053 | 24,145802 | 24,818953 |
| **POFUT2** | 25,549936 | 25,86848 | 25,189741 | 25,705408 |
| **POMGNT1** | 24,978811 | 25,164923 | 24,92795 | 25,902498 |
| **POMT1** | 25,244865 | 25,43993 | 25,143774 | 25,918856 |
| **POMT2** | 24,51996 | 24,855947 | 24,54353 | 24,918465 |
| **PRKCSH** | 22,628942 | 22,97715 | 22,546513 | 23,010626 |
| **ST3GAL1** | 25,5787 | 26,006802 | 25,667625 | 26,13306 |
| **ST3GAL2** | 24,994663 | 25,336723 | 24,786835 | 25,386112 |
| **ST6GAL1** | 23,833967 | 24,20171 | 24,388405 | 24,881487 |

| | | | | |
|---|---|---|---|---|
| **ST6GALNAC1** | Undetermined | Undetermined | Undetermined | 35,644268 |
| **ST8SIA2** | Undetermined | Undetermined | Undetermined | Undetermined |
| **ST8SIA3** | Undetermined | Undetermined | Undetermined | 38 |
| **ST8SIA4** | 29,76247 | 29,974627 | 28,850048 | 29,118605 |
| **ST8SIA6** | 31,701342 | 31,941397 | 31,86753 | 32,224792 |
| **UGGT1** | 24,955675 | 25,223888 | 24,951708 | 25,269278 |
| **UGGT2** | 26,4973 | 26,652733 | 26,494148 | 26,894848 |
| **GAPDH** | 18,602928 | 18,9723 | 17,866842 | 18,287085 |
| **HPRT1** | 23,014235 | 22,96646 | 23,510065 | 23,462599 |
| **GUSB** | 22,703266 | 22,764353 | 22,817125 | 22,848595 |
| **ACTB** | 19,661665 | 19,409184 | 19,500893 | 20,378485 |
| **B2M** | 19,057848 | 18,950157 | 19,778013 | 19,610174 |
| **HBMS** | 24,367435 | 24,680597 | 24,7739 | 24,824446 |
| **IPO8** | 25,482344 | 25,836906 | 25,824108 | 25,94232 |
| **PGK1** | 19,852783 | 20,397388 | 20,724718 | 20,51253 |
| **RPLP0** | 18,515245 | 18,913076 | 18,267073 | 18,314573 |
| **TBP** | 25,553478 | 25,990921 | 25,293953 | 25,59446 |
| **TFRC** | 22,15973 | 22,73112 | 22,496355 | 22,976725 |

## ANNEX 4

**Table 7.5 – Fold Change values obtained for each target in each array.** "Undetermined" states for the genes that were not amplificated; Statistical significance is represented with *.

| TARGET GENE | MDA-MB-231 (1) | MDA-MB-231 (2) | MDA-MB-231/1000NM (1) | MDA-MB-231/1000NM (2) |
|---|---|---|---|---|
| **18S** | -1,915 | 1,915 | -1,976 | -3,155 |
| **A4GNT** | Undetermined | Undetermined | Undetermined | Undetermined |
| **AGA** | 1,058 | -1,058 | 1,330 | 1,517 |
| **B3GLCT** | 1,036 | -1,036 | 1,424 | 1,682 |
| **B3GNT2** | -1,008 | 1,008 | 1,331 | 1,577 |
| **B3GNT3** | 1,034 | -1,034 | 1,903 | 2,088 |
| **B3GNT4** | -1,008 | 1,008 | 2,760 | 3,044 |
| **B3GNT8** | -1,030 | 1,030 | -1,066 | -1,236 |
| **B4GALT1** | 1,093 | -1,093 | 1,788 | 1,770 |
| **B4GALT2** | 1,050 | -1,050 | 1,384 | 1,312 |
| **B4GALT3** | 1,101 | -1,101 | 1,617 | 1,617 |
| **B4GALT5** | 1,051 | -1,051 | 1,265 | 1,265 |
| **CIGALT1** | -1,091 | 1,091 | 1,227 | 1,407 |
| **CIGALT1C1** | 1,065 | -1,065 | 1,587 | 1,349 |
| **EDEM1** | 1,056 | -1,056 | -1,243 | -1,340 |
| **EDEM2** | 1,005 | -1,005 | 1,374 | 1,396 |
| **EDEM3** | 1,095 | -1,095 | -1,148 | -1,169 |
| **FUCA1** | 1,001 | -1,001 | 1,090 | -1,291 |
| **FUCA2** | 1,025 | -1,025 | 1,066 | -1,395 |
| **FUT11** | 1,031 | -1,031 | -1,132 | -1,288 |
| **FUT8** | -1,032 | 1,032 | -1,065 | -1,148 |
| **GALNT1** | 1,035 | -1,035 | 2,273 | 2,300 |
| **GALNT10** | 1,071 | -1,071 | 1,017 | -1,242 |
| **GALNT11** | -1,020 | 1,020 | 1,095 | -1,725 |
| **GALNT12** | 1,059 | -1,059 | 2,069 | 1,345 |
| **GALNT13** | 1,064 | -1,064 | 1,260 | -1,650 |
| **GALNT14 *** | 1,298 | -1,298 | -558,969 | -544,330 |
| **GALNT2** | 1,037 | -1,037 | 1,015 | -2,316 |
| **GALNT3** | 1,094 | -1,094 | -1,138 | -1,782 |
| **POC1B-GALNT4,GALNT4** | 1,033 | -1,033 | 1,211 | -1,308 |
| **GALNT6** | 1,107 | -1,107 | 1,234 | -1,480 |
| **GALNT7** | 1,088 | -1,088 | 1,416 | -1,326 |
| **GALNT8** | Undetermined | Undetermined | Undetermined | Undetermined |
| **GALNT9** | Undetermined | Undetermined | Undetermined | Undetermined |
| **GALNT16** | 1,115 | -1,115 | 3,969 | 1,196 |
| **GALNTL5** | Undetermined | Undetermined | Undetermined | Undetermined |

| | | | | |
|---|---|---|---|---|
| **GALNTL6** | Undetermined | Undetermined | Undetermined | Undetermined |
| **GANAB** | 1,022 | -1,022 | 1,371 | -1,182 |
| **GCNT1** | -1,010 | 1,010 | 1,609 | 1,143 |
| **GCNT3** | -1,052 | 1,052 | 4,376 | 3,131 |
| **GCNT4** | 1,075 | -1,075 | 2,199 | 1,631 |
| **GLB1** | 1,085 | -1,085 | 1,180 | -1,153 |
| **GNPTAB** | 1,002 | -1,002 | 1,309 | -1,126 |
| **GNPTG** | 1,073 | -1,073 | 1,171 | -1,213 |
| **HEXA** | 1,102 | -1,102 | 1,612 | -1,013 |
| **HEXB** | -1,038 | 1,038 | 1,112 | -1,131 |
| **MAN1A1** | -1,001 | 1,001 | 1,177 | 1,003 |
| **MAN1A2** | 1,070 | -1,070 | -1,180 | -1,693 |
| **MAN1B1** | 1,083 | -1,083 | 1,622 | -1,053 |
| **MAN1C1** | 1,271 | -1,271 | 3,107 | 2,099 |
| **MAN2A1** | 1,057 | -1,057 | 1,562 | 1,069 |
| **MAN2A2** | 1,056 | -1,056 | 1,387 | -1,176 |
| **MAN2B1** | 1,057 | -1,057 | 1,294 | -1,205 |
| **MANBA** | 1,107 | -1,107 | 1,383 | -1,017 |
| **MGAT1** | -1,035 | 1,035 | 1,356 | -1,017 |
| **MGAT2** | 1,248 | -1,248 | 1,247 | -2,271 |
| **MGAT3 *** | 1,106 | -1,106 | 225,721 | 188,007 |
| **MGAT4A** | 1,029 | -1,029 | 3,066 | 2,385 |
| **MGAT4B** | -1,008 | 1,008 | 1,944 | 1,173 |
| **MGAT4C** | 1,353 | -1,353 | -1,718 | -1,318 |
| **MGAT5** | 1,159 | -1,159 | 1,173 | -1,090 |
| **MGAT5B** | 1,090 | -1,090 | 1,478 | -1,020 |
| **MOGS** | 1,070 | -1,070 | -1,223 | -2,001 |
| **NAGPA** | 1,102 | -1,102 | 2,004 | 1,293 |
| **NEU1** | 1,074 | -1,074 | 1,759 | 1,133 |
| **NEU2** | Undetermined | Undetermined | Undetermined | Undetermined |
| **NEU3** | 1,124 | -1,124 | 2,133 | 1,470 |
| **NEU4** | 1,145 | -1,145 | -1,013 | -1,241 |
| **OGT** | 1,085 | -1,085 | 2,151 | 1,607 |
| **POFUT1** | 1,146 | -1,146 | 1,377 | -1,158 |
| **POFUT2** | 1,117 | -1,117 | 1,577 | 1,103 |
| **POMGNT1** | 1,067 | -1,067 | 1,215 | -1,617 |
| **POMT1** | 1,070 | -1,070 | 1,262 | -1,356 |
| **POMT2** | 1,123 | -1,123 | 1,216 | -1,067 |
| **PRKCSH** | 1,128 | -1,128 | 1,314 | -1,050 |
| **ST3GAL1** | 1,160 | -1,160 | 1,200 | -1,151 |
| **ST3GAL2** | 1,126 | -1,126 | 1,430 | -1,059 |
| **ST6GAL1** | 1,136 | -1,136 | -1,175 | -1,654 |

| | | | | |
|---|---|---|---|---|
| **ST6GALNAC1** | Undetermined | Undetermined | Undetermined | Undetermined |
| **ST8SIA2** | Undetermined | Undetermined | Undetermined | Undetermined |
| **ST8SIA3** | Undetermined | Undetermined | Undetermined | Undetermined |
| **ST8SIA4** | 1,076 | -1,076 | 2,228 | 1,850 |
| **ST8SIA6** | 1,087 | -1,087 | 1,065 | -1,203 |
| **UGGT1** | 1,097 | -1,097 | 1,210 | -1,030 |
| **UGGT2** | 1,055 | -1,055 | 1,163 | -1,135 |